

Accepted Manuscript

Design, synthesis, and biological evaluation of cyclic-indole derivatives as anti-tumor agents via the inhibition of tubulin polymerization

Jun Yan, Jinhui Hu, Baijiao An, Li Huang, Xingshu Li



PII: S0223-5234(16)30792-9

DOI: [10.1016/j.ejmech.2016.09.056](https://doi.org/10.1016/j.ejmech.2016.09.056)

Reference: EJMECH 8922

To appear in: *European Journal of Medicinal Chemistry*

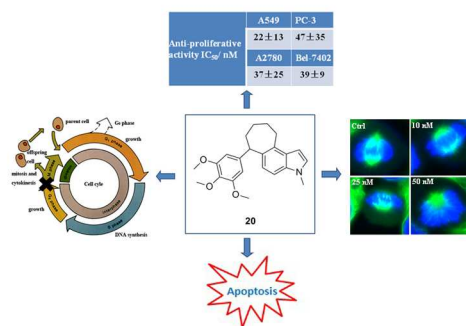
Received Date: 30 May 2016

Revised Date: 26 August 2016

Accepted Date: 18 September 2016

Please cite this article as: J. Yan, J. Hu, B. An, L. Huang, X. Li, Design, synthesis, and biological evaluation of cyclic-indole derivatives as anti-tumor agents via the inhibition of tubulin polymerization, *European Journal of Medicinal Chemistry* (2016), doi: 10.1016/j.ejmech.2016.09.056.

This is a PDF file of an unedited manuscript that has been accepted for publication. As a service to our customers we are providing this early version of the manuscript. The manuscript will undergo copyediting, typesetting, and review of the resulting proof before it is published in its final form. Please note that during the production process errors may be discovered which could affect the content, and all legal disclaimers that apply to the journal pertain.



Design, synthesis, and biological evaluation of cyclic-indole derivatives as anti-tumor agents via the inhibition of tubulin polymerization

Jun Yan, Jinhui Hu, Baijiao An, Li Huang, Xingshu Li*

Institute of Drug Synthesis and Pharmaceutical Process, School of Pharmaceutical Sciences, Sun Yat-sen University, Guangzhou 510006, China

ABSTRACT: This study revealed a new attractive cyclic-indole scaffold for the discovery of mitosis-targeting anti-tumour agents. Among all of the synthesised derivatives, compound **20** displayed the most potent anti-proliferative activity (with IC_{50} values of 22 - 56 nM against seven cancer cell lines) and tubulin polymerization inhibition ($IC_{50} = 0.15 \pm 0.07 \mu M$), which were much better than those of the reference compound Combretastain A-4 (CA-4). High selectivity ratios (9.68-7.61) of compound **20** toward human normal cells and cancer cells were also observed. Immunofluorescence assay elucidated that compound **20** disrupted the intracellular microtubule network and interfered with cell mitosis. Cellular mechanism studies demonstrated that compound **20** arrested the cell cycle at the G_2/M phase and induced apoptosis in a time- and dose-dependent manner. In summary, compound **20** deserves consideration for in vivo anti-tumour evaluation in further studies.

KEYWORDS: cyclic-indole derivatives, antiproliferative activity, tubulin polymerization inhibitor, cell cycle arrest, apoptosis

1. Introduction

Microtubules are long, hollow cylinders that are mainly composed of α - and β -tubulin

Abbreviations: CA-4, Combretastain A-4; VDAs, vascular disrupting agents; HMTA, hexamethylenetetramine; HUVECs, human umbilical vein endothelial cells; SARs, structure and activity relationships; SD, standard error; PI, propidium iodide; HR-MS, high resolution mass spectra.
For X. Li.: Tel.: +086-20-3994-3050; Fax: +086-20-3994-3050; e-mail: lixsh@mail.sysu.edu.cn

dimers; and γ -tubulin plays a major role in the nucleation of microtubule assembly.[1] These tubulin dimers polymerize end-to-end to form a protofilament.[2] Microtubules continuously keep a state of dynamic equilibrium to exert their structural function.[3, 4] The tubulin-microtubule system is an important intracellular framework, which plays a pivotal role in the maintenance of cell structure, regulation of motility, and cell division.[2, 5, 6] Consequently, it has become an attractive target for the design of new antimitotic agents for cancer therapy.[7-9] Antimitotic agents currently used in the clinic are mainly classified into two broad categories: vinca alkaloids (represented by vincristine and vinorelbine), which inhibit microtubule polymerization and taxoids (represented by a family of taxanes), which promote microtubule polymerization.[10] Colchicine was the first drug reported to function as the tubulin polymerization inhibitor in the late 1930s.[11] Combretastatin A-4 (CA-4, Figure 1) is another potent antimitotic agent, which was first isolated from the African bush willow *Combretum caffrum*, and exhibits strong cytotoxicity against a variety of cancer cells.[12] The encouraging antitumour profile of CA-4 has inspired many medicinal chemists' extensive interest in the design and synthesis of CA-4 analogues.[13-16] Most of the reported modifications involved stabilizing the conformation of the olefinic bridge using different substitutions or replacing the 3-hydroxy-4-methoxyphenyl moiety of CA-4 with other biologically active entities.[17] The *cis* double bond of CA-4 is easy to isomerize to the more thermodynamically stable, but less bioactive, *trans* isomers. In this case, numerous modifications, which on one hand aimed to stabilize the conformation of CA-4 by replacing the olefinic bridge with different cyclic moieties and on the other hand to retain its biological activity, were under extensive investigation.[18, 19] Pinney and co-workers described the discovery of the benzosuberene analog **1** (Figure 1) as a potent tubulin polymerization inhibitor,[20] and then established various functionalized benzosuberene analogues for further evaluation as promising anti-cancer agents.[21-23] Meantime, Maderna and other groups also obtained new benzosuberene analogues with structural modifications on the B-ring as cytotoxicity agents.[24, 25] Considering the extensive pharmacological activities of the indole-based compounds, Pinney and other groups developed novel

indole-based inhibitors of tubulin polymerization[26-29] and compound Oxi8006[30] was one of the most representative agent which demonstrated pronounced interference with tumor vasculature in a preliminary *in vivo* study.[31] In the previously work, the seven membered ring of compound **1** was substituted with heterocyclic part to obtain compound **2** (Figure 1) which displayed excellent anti-tumor activity *in vitro* and *in vivo*. [32] In recent years, our group has also been committed to the design and synthesis some indole-based compound **3**[33] (Figure 1) and indole-chalcone derivative **4**[34] (Figure 1) as novel tubulin polymerization inhibitors. Inspired by the work of Pinney and others, we fused benzosuberenes with indole-based part to obtain a novel series of cyclic-indole derivatives. Preliminary biochemical evaluation in terms of inhibition of tubulin polymerization along with anti-proliferative activity study toward various types of cancer cells, analysis of structure-activity relationships, and elucidation of the molecular mechanism are presented.

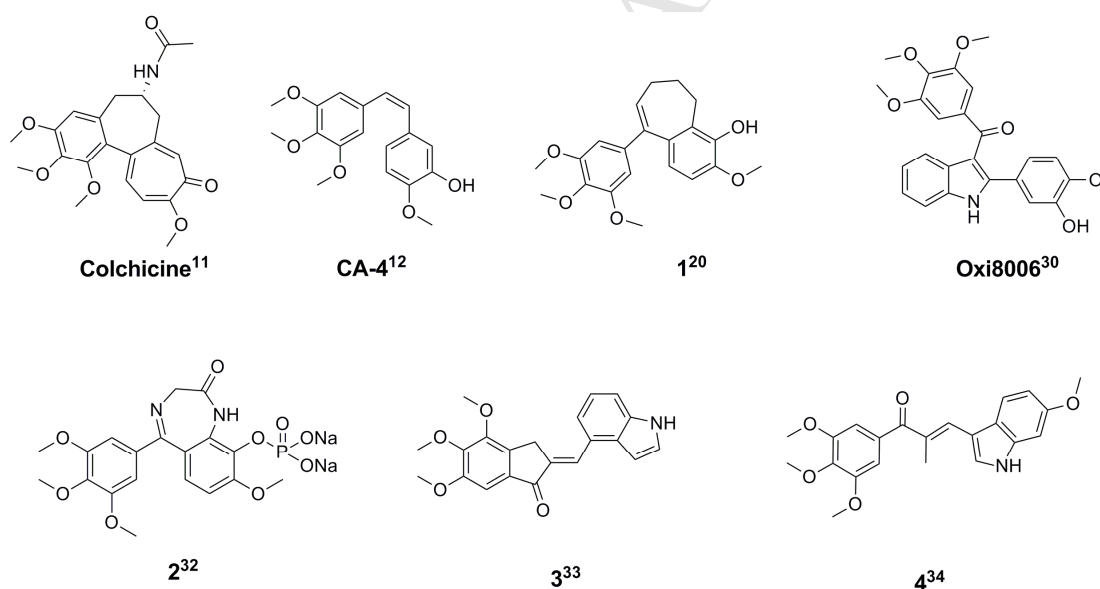


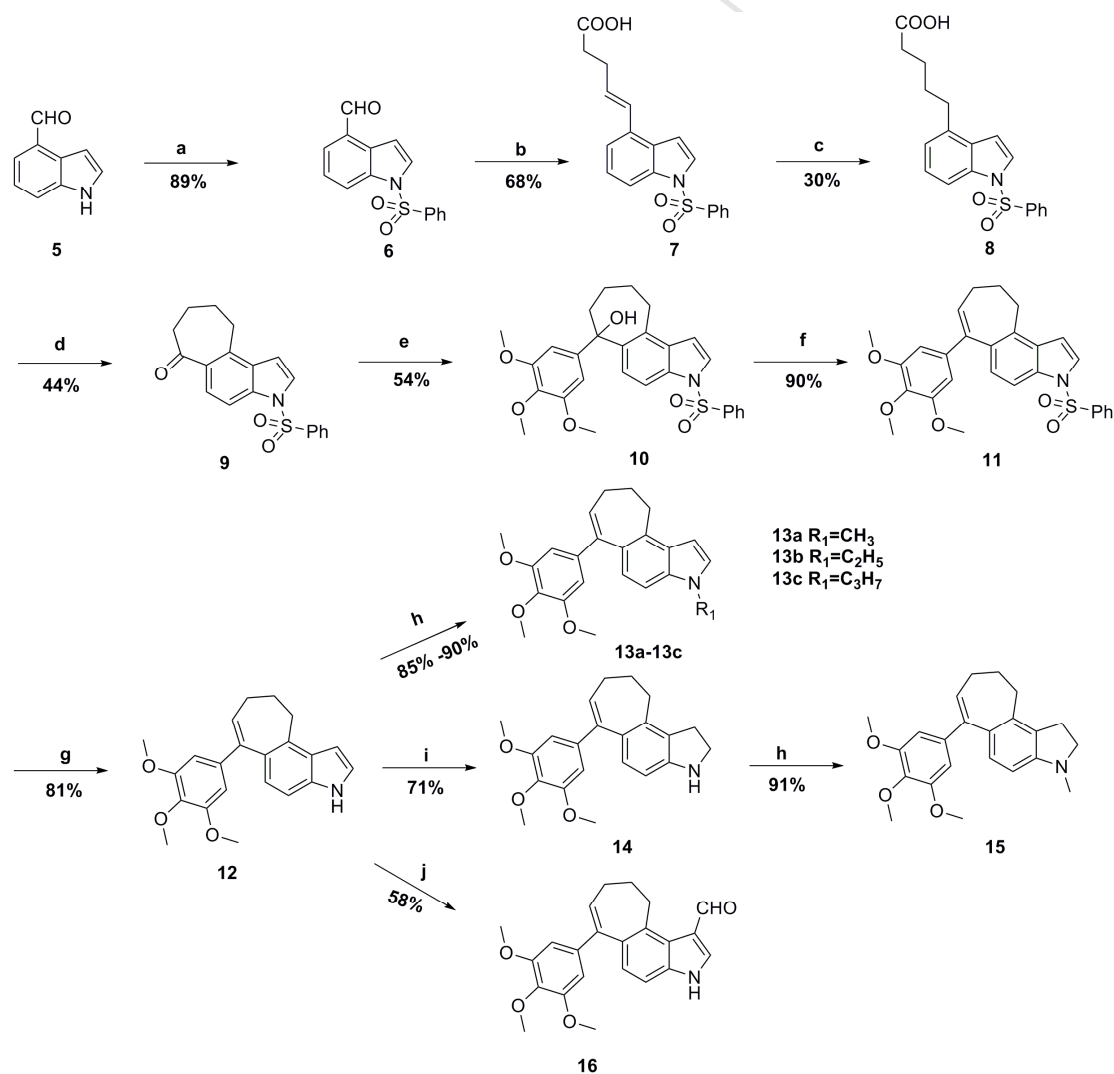
Figure 1. Structures of the representative tubulin polymerization inhibitors and vascular disrupting agents (VDAs).

2. Results and Discussion

2.1 Chemistry

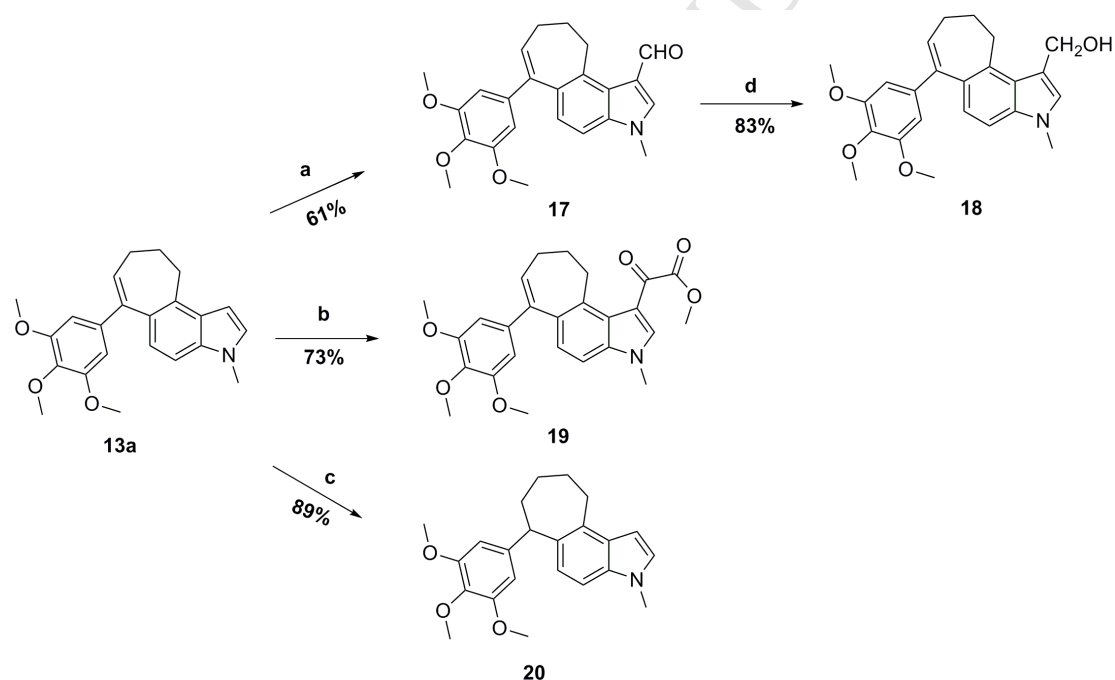
The synthetic routes for the cyclic-indole derivatives are outlined in Schemes 1-3. Using the N-benzenesulfonyl-protected starting material **6**, the Wittig reaction in the presence of a strong base (NaHMDS) produced the aryl pentenoic acid **7**. [35, 36] The

intermediate **7** was then subjected to a hydrogenation and intramolecular Friedel–Crafts acylation afforded cyclohepta-indolone **9**. The reaction of **9** with a lithium reagent in situ prepared from 5-bromo-1,2,3-trimethoxybenzene and *n*-BuLi provides cyclohepta-indolol **10**. A good yield of cyclohepta-indole derivative **11** was easily obtained from the dehydration of **10** in the presence of an acid.[20] Deprotection of the cyclohepta-indole **11** in the solution of KOH in methanol afforded cyclohepta-indole **12**. The modification of intermediate **12** by *N*-alkylation produced compounds **13a** - **13c**. Treatment intermediate **12** with sodium cyanoborohydride in acid conditions yielded the indoline **14**. The methylation of indoline **14** with iodomethane afforded methyl indoline **15**. Indole-aldehyde **16** was obtained from indole **12** using the Duff reaction in the presence of hexamethylenetetramine (HMTA) (Scheme 1).



Scheme 1. Reagents and conditions: (a) benzenesulfonyl chloride, KOH, TBAHS, CH₂Cl₂, room temperature; (b) (i) (3-carboxypropyl)triphenylphosphonium bromide, NaHMDS, THF, -20 °C; (ii) aldehyde, **6**, -78 °C, 18 h; (c) Pd/C, H₂, MeOH; (d) Eaton's Reagent: 7.7% (w/w) P₂O₅ in methanesulfonic acid, room temperature; (e) (i) 5-bromo-1,2,3-trimethoxybenzene, n-BuLi, THF; (ii) ketone, **9**, -78 °C, 12 h; (f) p-toluenesulfonic acid, CHCl₃; (g) 1 M KOH, MeOH; (h) CH₃I / C₂H₅Br / C₃H₇Br, NaH, THF; (i) NaBH₃CN, CH₃COOH; (j) Hexamethylenetetramine, CH₃COOH, N₂.

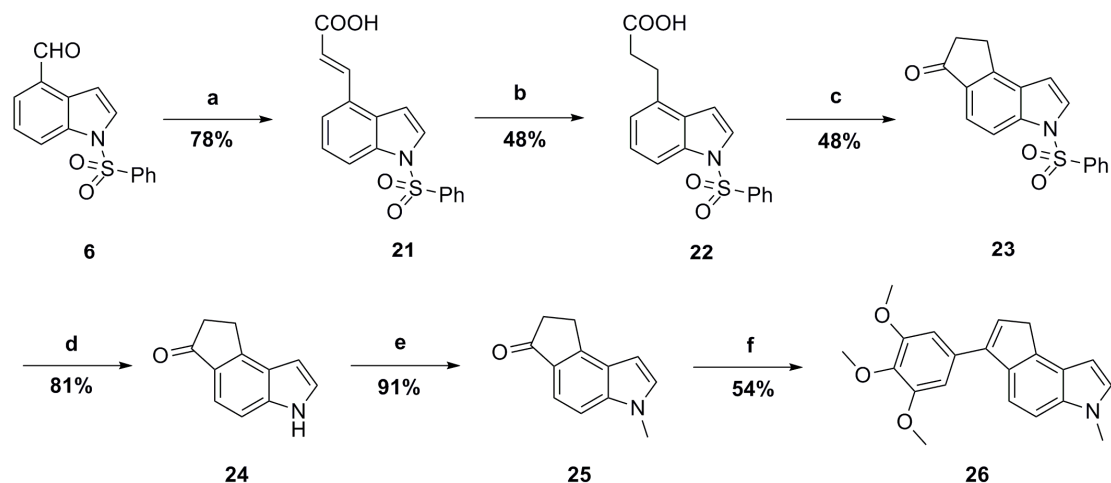
Under the same conditions, aldehyde **17** was readily produced from N-methylated indole **13a**. Reduction of aldehyde **17** with sodium borohydride afforded indolyl methanol **18**. **13a** was treated with oxalyl chloride to afford intermediate oxoacetyl chloride. Then the mixture was immediately quenched by methanol to obtain oxoacetate **19**. Reduction of the double bond of olefin **13a** gave alkane **20** (Scheme 2) with a good yield.



Scheme 2. Reagents and conditions: (a) Hexamethylenetetramine, CH₃COOH, N₂; (b) (i) oxalyl chloride, Et₂O; (ii) CH₃OH, Et₃N; (c) H₂, Pd/C, CH₃OH; (d) NaBH₄, CH₃OH.

Simultaneously with the synthesis of cyclohepta-indoles, the hepta-cyclic nucleus was also replaced by the five-cyclic skeleton. Similarly, acrylic acid **21** was prepared with good yield using the Knoevenagel condensation reaction with malonic acid and the starting material **6**. The following hydrogenation and cyclization produced the indolone **23** with an acceptable yield. Cyclopenta-indolone **25** was easily obtained by

deprotection and then methylation of the indolone **23**. Treating **23** with a lithium reagent, prepared as described above at $-78\text{ }^{\circ}\text{C}$, yielded cyclopenta-indole **26** by sequentially treating the reaction mixture with aqueous NH_4Cl at room temperature (Scheme 3).



Scheme 3. Reagents and conditions: (a) malonic acid, piperidine, pyridine; (b) Pd/C, H_2 , MeOH; (c) methanesulfonic acid, P_2O_5 , room temperature; (d) 1 M KOH, MeOH; (e) CH_3I , NaH, THF; (f) (i) 5-bromo-1,2,3-trimethoxybenzene, n-BuLi, THF; (ii) ketone, **25**, $-78\text{ }^{\circ}\text{C}$, 12 h.

2.2 *In vitro* antiproliferative activity

In the initial screening of the antiproliferative activity, seven human cancer cell lines derived from various tissues and organs were chosen including the non-small cell lung cancer cell line A549, human epithelial cervical cancer cell line HeLa, human prostate cancer line PC-3, human liver carcinoma cell line Bel-7402, human colon cancer cell line Lovo, human ovarian cancer cell line A2780, and human breast carcinoma cell line MCF-7. Evaluation of the antiproliferative activity was carried out using the MTT (3-(4,5-dimethylthiazol-2-yl)-2,5-diphenyltetrazolium bromide) assay. The data in Table 1 indicate that the length of the alkyl chain at the N-1 position of the indole ring was obviously related to the anti-proliferative activity. Comparing the activity of compounds **12** (IC_{50} range from 0.45 to 1.56 μM) and **13a** (IC_{50} range from 0.044 to 0.093 μM), the N-methylation was indeed favourable for the anti-proliferative activity. Moreover, when the R_1 group was replaced by a methyl group or an ethyl group, both compounds **13a** and **13b** displayed similar potent activities. However, extending the carbon chain to a propyl group resulted in a 7.27- to 17.7-fold decrease in the anti-proliferative activities.

Next, the effects of different substitutions on the 3-position of the indole ring were also investigated. As shown in Table 1, when R₂ was replaced by an aldehyde group or hydroxymethyl group, compounds **17** and **18** nearly retained the excellent anti-proliferative activities towards all of the tested cancer cell lines, while the replacement with oxoacetyl group (compound **19**) led to the absolute loss of activity. Moreover, the difference in anti-proliferative activities between compounds **16** and **17** further evidenced the importance of the N-methylation.

To elucidate the structure and activity relationships (SARs) in more detail, we investigated whether the double bond of the indole ring and hepta-cyclic ring were indispensable for the anti-proliferative activity. After the double bond of the indole ring and hepta-cyclic ring were reduced, the targeted compounds **15** and **20** also displayed potent anti-proliferative activities. However, reducing the size of the hepta-cyclic ring to the five-cyclic skeleton (compound **26**) caused nearly a 3.04- to 7.19-fold decrease in the anti-proliferative activities compared to the corresponding compound **13a**.

Table 1. Antiproliferative activity of compounds against seven human cancer cell lines^a

Compd.	IC ₅₀ mean±SD (μM) ^b						
	A549	HeLa	PC-3	Bel-7402	Lovo	A2780	MCF-7
12	0.451±0.13	0.79±0.08	0.98±0.13	0.62±0.29	0.52±1.36	1.01±1.29	1.56±1.46
13a	0.049±0.023	0.056±0.017	0.093±0.025	0.078±0.031	0.047±0.013	0.044±0.012	0.069±0.021
13b	0.056±0.031	0.061±0.014	0.085±0.036	0.066±0.014	0.039±0.015	0.032±0.023	0.079±0.026
13c	0.52±0.03	0.60±0.02	0.69±0.12	0.48±0.23	0.69±0.17	0.24±0.09	0.78±0.31
14	0.312±0.242	0.701±0.16	0.741±0.09	0.797±0.321	1.123±0.231	0.597±0.159	0.812±0.452
15	0.056±0.009	0.045±0.014	0.077±0.021	0.061±0.011	0.079±0.037	0.069±0.038	0.058±0.029
16	0.47±0.57	0.86±0.12	0.95±0.23	1.26±0.74	1.13±0.15	1.02±0.39	2.06±1.17
17	0.029±0.014	0.041±0.027	0.031±0.013	0.049±0.029	0.052±0.021	0.033±0.011	0.059±0.019
18	0.043±0.002	0.033±0.015	0.049±0.021	0.046±0.009	0.032±0.017	0.031±0.019	0.063±0.022
19	>10	>10	>10	>10	>10	>10	>10

20	0.022±0.013	0.056±0.019	0.047±0.035	0.039±0.009	0.049±0.033	0.037±0.025	0.051±0.041
26	0.149±0.091	0.326±0.129	0.412±0.014	0.561±0.138	0.297±0.112	0.186±0.021	0.449±0.127
CA-4	0.010±0.001	0.012±0.001	0.026±0.009	0.013±0.006	0.017±0.002	0.016±0.002	0.029±0.004

^aCell lines were treated with different concentrations of the compounds for 48 h. Cell viability was measured by MTT assay as described in the Experimental Section. ^bIC₅₀ values are indicated as the mean±SD (standard error) of at least three independent experiments.

2.3 *In vitro* inhibition of tubulin polymerization

Considering the critical role of microtubules in cell architecture, such as cell mitosis, cell shape maintenance and protein transportation, we also evaluated the inhibitory efficacy of these cyclic-indole derivatives on microtubule assembly *in vitro*. According to the method originally described by Bonne *et al.*, [37] the tested compounds were incubated with un-polymerized pure porcine tubulin, and the polymerization was monitored by the change of fluorescence intensity. In the control group, tubulin polymerization had indeed occurred as evidenced by an enhancement of the fluorescence intensity along with time extension. When incubated with the tested compounds at the indicated concentrations, the increased tendency of the fluorescence intensity was slowed down or absolutely suppressed at higher concentrations. On the base of the antiproliferative activity screening, compounds **13a**, **15**, **17**, **18**, **20**, which bore representative structures and displayed excellent antiproliferative activities, were primarily chosen for the tubulin polymerization evaluation. The IC₅₀ values of compounds **13a**, **15**, **17**, **18**, and **20** listed in Table 2 showed that these compounds are potent tubulin polymerization inhibitors and more potent than reference compound CA-4. Since compound **20** displayed excellent anti-proliferative activity and the best tubulin polymerization inhibitory activity in the

initial screening, we selected it as the optimized compound for the following further studies.

Table 2. Effects of the selected compounds on tublin polymerization inhibition

Compd.	13a	15	17	18	20	CA-4
IC ₅₀ /μM ^a	0.58 ± 0.12	1.04 ± 0.18	0.47 ± 0.02	0.41 ± 0.14	0.15 ± 0.07	1.12 ± 0.05

^aIC₅₀ values are indicated as the mean±SD (standard error) of three independent experiments.

2.4 Selectivity of compound 20 towards normal cells and cancer cells.

Considering the high cytotoxicity of chemotherapeutic agents, their selectivity towards normal cells and cancer cells is particularly important. To evaluate the selectivity of the optimal compound 20 towards human normal cells and cancer cells, four types of non-tumorigenic cell lines from different origins were used, including HUVECs (human umbilical vein endothelial cells), MCF-10A (human mammary epithelial cell line), BJ (human dermal fibroblasts), and HLF (human embryonic lung fibroblast cell line). The results summarized in Table 3 showed that 20 was associated with a high cytotoxicity towards A549 cells and a relatively low toxicity towards human normal cells, which exhibited 9.68-, 30.5-, 55.0-, and 76.1-fold selectivity ratios for quiescent HUVECs, MCF-10A, BJ, and HLF cells, respectively. In order to elucidate the results of the reduced cytotoxicity against HUVECs, we performed a contemporaneous microscopy study using A549 cells and HUVECs cells treated with compound 20 at 20 nM and 200nM (IC₅₀ concentrations). As shown in Figure S VI (supporting information), treated with compound 20 nM for 48 h, the A549 cells displayed obvious cell morphology alteration such as cell rounding, cell shrinkage, membrane blebbing and loss of adherent property, which well indicated the cytotoxicity of compound 20. Moreover, this morphology changes were more apprent at 200 nM treatment. While, treated at the same condition, the HUVECs cells did not exhibit any cell damages at 20 nM and displayed a certain extent of damage at 200 nM. Along with the results of MTT assay (Table 3), these results well demonstrated the

reduced cytotoxicity against HUVECs. The tremendous role of microtubules in cell division makes it a fascinating target for anticancer drugs. Compared to the normal cells, cancer cells have a rapid proliferation characteristics of division which highly depend on microtubule dynamic equilibrium.[38] Thus, cancer cells are more sensitive to microtubules-destabilizing agents, which might explain the apparent selectivity of compound **20** toward A549 cells and four normal cell lines.

Table 3. The selectivity ratio of compound **20** toward human normal cells and cancer cells.

	IC ₅₀ , ^a mean ± SD (μM)	Selectivity ratio ^c
A549	0.022 ± 0.013	
Quiescent HUVECs ^b	0.213 ± 0.017	9.68
MCF-10A	0.672 ± 0.156	30.5
BJ	1.211 ± 0.224	55.0
HLF	1.674 ± 0.538	76.1

^aData are presented as the mean ± SE from the dose-response curves of at least three independent experiments. ^bFor quiescent growth conditions, HUVECs were cultured in endothelial cell medium containing 0.5% fetal calf serum and in absence of growth factor. ^cSelectivity ratio = (IC₅₀ human normal cells) / (IC₅₀ A549).

2.5 Disruption of intracellular microtubule dynamics

Microtubules, which consist of α -, β -tubulin heterodimers, are key components of the mitotic spindle and always sustain the dynamic balance to maintain its biological function.[39] Since the tubulin polymerization inhibitory effect of **20** has been verified in vitro, we subsequently performed the immunofluorescence assay to observe its effect on the intracellular microtubule system. As shown in Figure 2, compound **20** disrupted the cellular microtubule network and disturbed the cell mitosis. The nucleus and microtubules in the vehicle-treated group appeared as normal state as characterized by the slim and fibrous microtubules, well-organized structure surrounding the uncondensed nucleus, and spindles present during bipolar

mitotic division. However, with increasing compound concentrations, the meshy microtubule networks were heavily shrunk around the nucleus, and monopolarization or multipolarization of the spindle and multinucleation phenomena were easily observed, which indicated that compound **20** disrupted microtubule organizations and interfered with the mitosis of A549 cells.

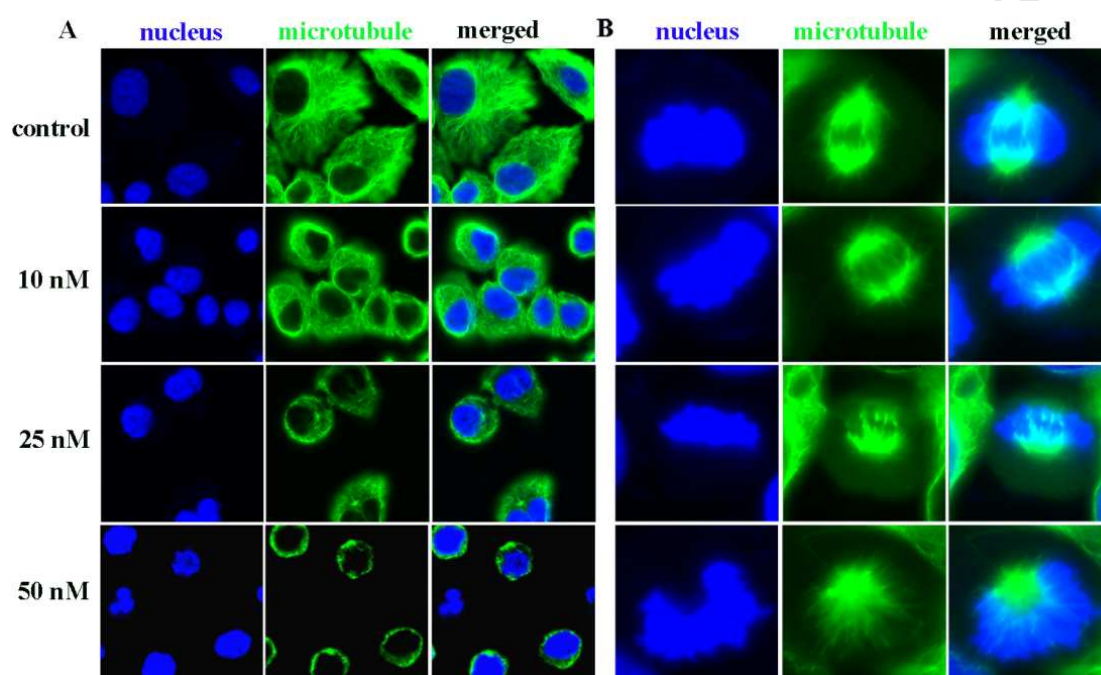


Figure 2. Disruption effect of compound **20** on the cellular microtubule network (A) and cell mitosis (B) visualized by immunofluorescence. A549 cells were plated in confocal dishes and exposed to **20** at the indicated concentrations for 24 h. Then, the cells were fixed and processed to study the immunofluorescence of microtubules (stained with primary β -tubulin mouse antibody and Alexa Fluor 488 goat anti-mouse IgG antibody, green) and nuclei (stained with Hoechst 33342, blue) using an LSM 570 laser confocal microscope (Carl Zeiss, Germany) as described in the Experimental Section. Magnification: $\times 64$ (A), $\times 100$ (B). The experiments were performed three times, and the results of representative experiments are shown.

2.6 Cell cycle analysis

As most microtubule polymerization inhibitors disrupt cell mitosis and exert cell cycle arrest effects,[40] we applied flow cytometry to analyse the cell cycle arrest effect of compound **20**. As shown in Figure 3, **20** caused significant cell cycle arrest at the G₂/M phase in a dose- and time-dependent manner with concomitant losses of G₁ phase cells. When treated with **20** at 10, 25, and 50 nM for 24 h, the percentages of cells arrested at the G₂/M phase were 41.0%, 55.1%, and 72.1%, respectively. After a 48 h treatment, the remarkable accumulation of cells arrested in the G₂/M phase was more obvious. These results demonstrated that **20**, similar to most tubulin polymerization inhibitors, disrupted the dynamic balance of the tubulin-microtubule system and further blocked the cell cycle distribution at the G₂/M phase.

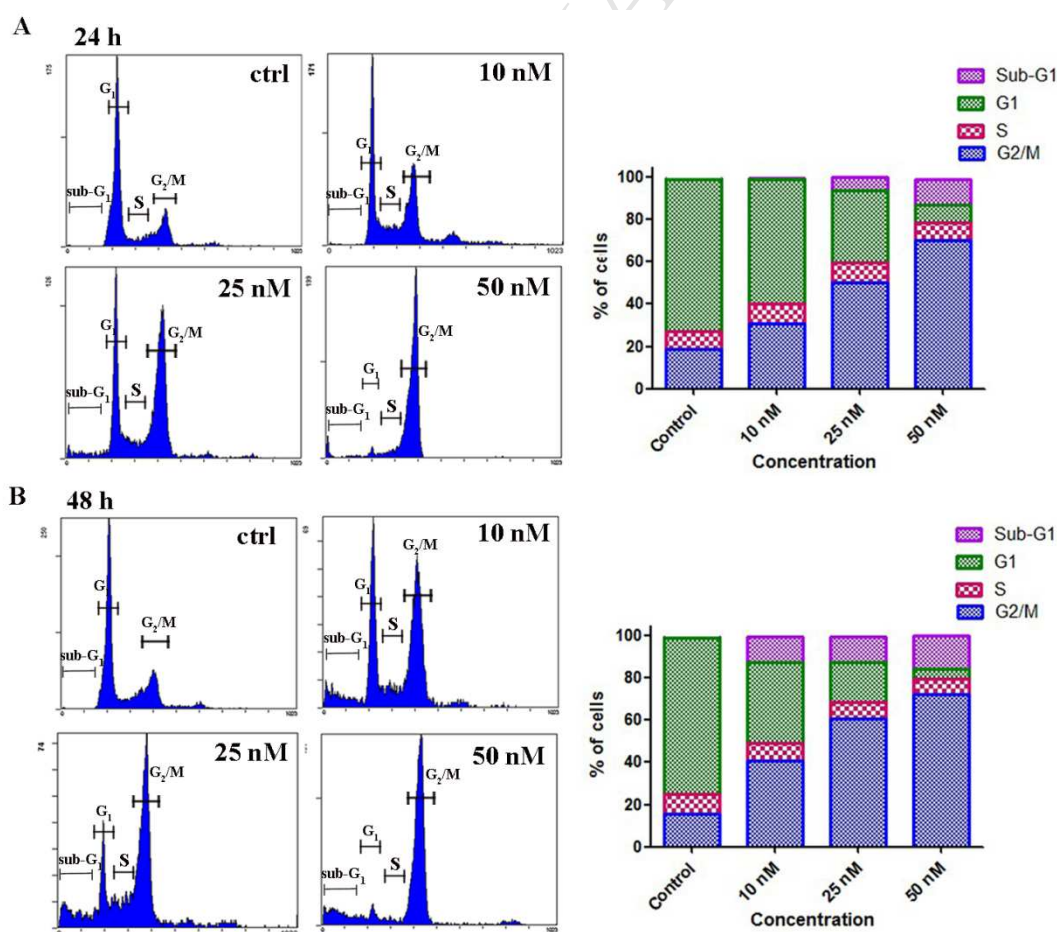


Figure 3. Compound **20** arrested cell cycle progression at the G₂/M phase in a dose- and

time-dependent manner. The A549 cells were treated with compound **20** at 10, 20, or 50 nM for 24 h (A) or 48 h (B). Quantitative analysis of the percentage of cells in each cell cycle phase were analysed by EXPO32 ADC analysis software. The experiments were performed three times, and the results of representative experiments are shown.

2.7 Cell apoptosis analysis

According to the cell cycle analysis results above, it was assumed that compound **20** treatment induces cell apoptosis, which was evidenced by the appearance of the characteristic hypodiploid DNA content peak (sub-G1) (Figure 5B). To confirm this hypothesis, A549 cells were treated with various concentrations of compound **20** for 24 or 48 h and then were harvested, stained with Annexin V-FITC/PI and monitored by flow cytometry. As shown in Figure 4, compound **20** induced A549 cell apoptosis in a dose- and time-dependent manner. The percentage of apoptotic cells after the 24 h treatment was only 0.63% in the control group. The early and late apoptotic cells increased to 22.8%, 39.6%, and 59.8% after 24 h of 10, 20, and 50 nM of compound **20** treatment, respectively, whereas after a 48 h incubation, the percentages of the early and late apoptotic cells were strikingly increased to 41.4%, 58.4%, and 60.2%, respectively. Moreover, after the 48 h incubation, most cells treated at the highest concentration underwent late apoptosis. These data demonstrate that compound **20** effectively induced cell apoptosis in A549 cells in a dose- and time-dependent manner, eventually leading to cell death.

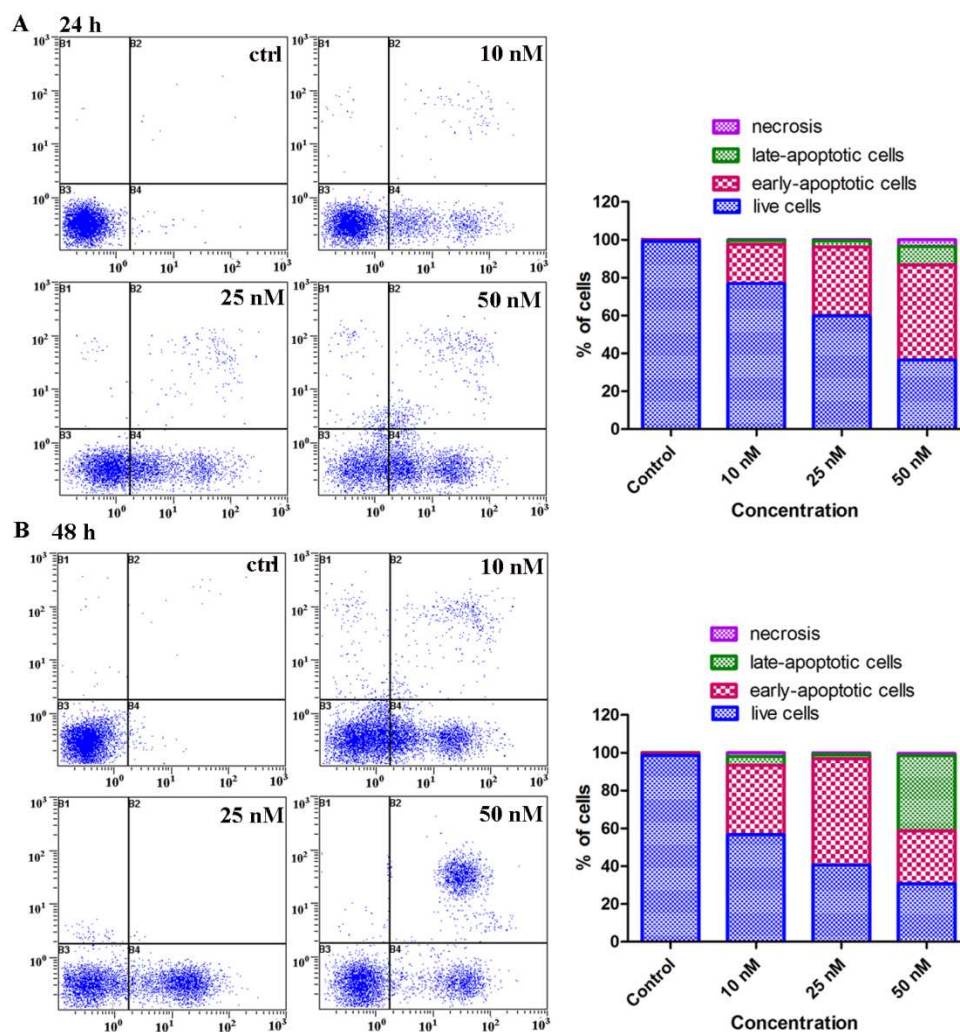


Figure 4. Compound **20** induced A549 cell apoptosis in a dose- and time-dependent manner. The A549 cells were treated with compound **20** at 10, 20, or 50 nM for 24 h (A) or 48 h (B). The percentages of cells in each stage of cell apoptosis were quantified by flow cytometry: (upper left quadrant) necrosis cells; (upper right quadrant) late-apoptotic cells; (bottom left quadrant) live cells; and (bottom right quadrant) early apoptotic cells. The experiments were performed three times, and the results of representative experiments are shown.

3. Conclusions

In summary, we have designed, synthesized, and evaluated a series of novel cyclic-indole derivatives as tubulin polymerization inhibitors for cancer therapy. All of the designed compounds possessed potent anti-proliferative activities against seven

human cancer cell lines derived from different tissues and organs. Considering the pivotal role of the tubulin-microtubule system in cell division, the *in vitro* tubulin polymerization inhibitory activities were also evaluated. We discovered that these compounds, which demonstrated good anti-proliferative activities *in vitro*, also exhibited excellent tubulin polymerization inhibitory activities. The relatively low cytotoxicity of compound **20** further revealed the possibility for clinical application. Moreover, detection of the intracellular microtubule immunofluorescence confirmed that the potent antiproliferative activity of compound **20** was strongly related to its massive disruption and interference effect on microtubule network organization and cell mitosis. Furthermore, the mechanism study elucidated that compound **20** triggered cell cycle arrest at the G₂/M phase and induced cell apoptosis in a dose- and time-dependent manner. Taken altogether, compound **20** effectively inhibited tubulin polymerization, disrupted the intracellular tubulin-microtubule balance, and interfered with cell mitosis resulting in prolonged G₂/M cell cycle arrest and thus ultimately led to apoptosis of cancer cells. As a promising new tubulin-targeting agent, compound **20** is worth further *in vivo* antitumour evaluation as a potential chemotherapeutic agent.

4. Experimental Section

4.1 Chemistry

¹H NMR and ¹³C NMR spectra were acquired on a Bruker AvanceIII spectrometer with TMS as the internal standard. High resolution mass spectra (HR-MS) were recorded on an Agilent LC-MS 6120 instrument with an ESI mass selective detector in positive ion mode. Melting points were determined on an SRS-OptiMelt automated melting point instrument. The purity of the synthesized compounds was determined by high-performance liquid chromatography (HPLC) with a TC-C18 column (4.6 × 250 mm, 5 μm), an acetonitrile/water or methanol/water mobile phase, and a flow rate of 1.00 mL/min.

Synthesis of 1-(phenylsulfonyl)-1H-indole-4-carbaldehyde (**6**)[35]

After a suspension of 1H-indole-4-carbaldehyde **5** (2.0 g, 14 mmol), TBAHS (0.72 g, 2.1 mmol), and KOH (1.6 g, 28 mmol) in CH₂Cl₂ (100 mL) was stirred for 20 min, benzenesulfonyl chloride (2.6 mL, 21 mmol) was added, and the mixture was stirred at room temperature for 16 h. The reaction was quenched with water, and extracted with CH₂Cl₂ (50 mL × 3). The combined organic layer was dried over anhydrous MgSO₄ and concentrated under reduced pressure to give a yellow residue, which was purified by silica gel chromatography (ethyl acetate / petroleum = 1:8) to afford the 1-phenylsulfonyl indole (3.5 g, 12 mmol) as a white solid. Yield: 89%. ¹H NMR (400 MHz, CDCl₃) δ 10.17 (s, 1H), 8.28 (d, *J* = 8.3 Hz, 1H), 7.88 (d, *J* = 8.1 Hz, 2H), 7.77 (d, *J* = 2.8 Hz, 1H), 7.72 (d, *J* = 7.4 Hz, 1H), 7.59 – 7.42 (m, 6H).

Synthesis of (E)-5-(1-(phenylsulfonyl)-1H-indol-4-yl)pent-4-enoic acid (**7**)[36]

To a a suspension of (3-carboxypropyl)triphenylphosphonium bromide (0.92 g, 2.2 mmol) in THF (12 mL), NaHMDS (2.2 mL, 4.3 mmol) was added dropwise at temperature of -20 °C and the suspension and further stirred for 20 min. The mixture was cooled to -78 °C and then aldehyde **6** (0.57 g, 2.0 mmol) was added. After stirred for 18 h, the solvent was removed in vacuo and H₂O was added. The residue was extracted with diethyl ether and the H₂O layer was acidified to pH 2 using HCl (1 M). The acidified aqueous layer was extracted with ethyl acetate and the combined organic layers were dried over sodium sulfate, filtered and concentrated to dryness. The product was purified over silica gel using ethyl acetate: petroleum (1:1) to obtain the alkenoic acid (1.4 mmol, 0.48 g) as yellow oil. Yield: 68%. ¹H NMR (400 MHz, Chloroform-d) δ 7.92 – 7.82 (m, 3H), 7.58 (d, *J* = 3.7 Hz, 1H), 7.53 – 7.46 (m, 1H), 7.40 (t, *J* = 7.8 Hz, 2H), 7.32 – 7.21 (m, 2H), 6.81 (d, *J* = 3.5 Hz, 1H), 6.76 – 6.65 (m, 1H), 6.27 (dt, *J* = 15.9, 6.3 Hz, 1H), 2.56 (q, *J* = 5.6, 4.5 Hz, 4H).

Synthesis of 5-(1-(phenylsulfonyl)-1H-indol-4-yl)pentanoic acid (**8**)[35]

To a stirred suspension of **7** (0.71 g, 2.0 mmol) in methanol (10 mL), Pd / C (0.10 g) was added and the mixture was stirred under H₂ atmosphere at room temperature for 3 h. Then, the mixture was filtered and vacuumed to get colorless oil (0.21 g, 0.60 mmol). Yield: 30%. ¹H NMR (400 MHz, Chloroform-d) δ 7.88 (dd, *J* = 8.2, 1.0 Hz, 2H), 7.83 (d, *J* = 8.3 Hz, 1H), 7.57 (d, *J* = 3.7 Hz, 1H), 7.52 (t, *J* = 7.4 Hz,

1H), 7.43 (t, $J = 7.7$ Hz, 2H), 7.25 – 7.19 (m, 1H), 7.03 (d, $J = 7.4$ Hz, 1H), 6.70 (d, $J = 3.7$ Hz, 1H), 2.81 (t, $J = 7.1$ Hz, 2H), 2.36 (t, $J = 6.9$ Hz, 2H), 1.74 – 1.67 (m, 4H).

Synthesis of 3-(phenylsulfonyl)-7,8,9,10-tetrahydrocyclohepta[e]indol-6(3H)-one (9)[41]

To a rapidly stirred solution of phosphorus pentoxide:methanesulfonic acid (1:10, 10 g), compound **8** (1.0 g, 2.8 mmol) was added in small portions. After the mixture was stirred at room temperature for 4.0 h, 40 mL of water was added in drop wise and the aqueous mixture was stirred rapidly for 5-10 min to ensure the hydrolysis of methanesulfonic anhydride. The mixture was extracted with ethyl acetate, washed subsequently with dilute aqueous sodium bicarbonate and water, dried over anhydrous sodium sulfate, and concentrated in vacuum to provide the crude product, which was purified by chromatography on silica gel (4:1 of petroleum/ethyl acetate as an eluent) to afford the product (1.2 mmol, 0.42 g) as pink oil in 44% yield. ^1H NMR (400 MHz, Chloroform- d) δ 7.89 (d, $J = 3.0$ Hz, 3H), 7.74 (d, $J = 8.7$ Hz, 1H), 7.63 (d, $J = 3.8$ Hz, 1H), 7.55 (d, $J = 7.5$ Hz, 1H), 7.46 (t, $J = 7.7$ Hz, 2H), 6.81 (d, $J = 3.7$ Hz, 1H), 3.10 (d, $J = 6.4$ Hz, 2H), 2.78 – 2.74 (m, 2H), 1.91 (p, $J = 6.5$ Hz, 2H), 1.85 – 1.79 (m, 2H).

Synthesis of 3-(phenylsulfonyl)-6-(3,4,5-trimethoxyphenyl)-3,6,7,8,9,10-hexahydrocyclo-hepta[e]indol -6-ol (10)[20]

Under the argon atmosphere, the solution of 5-bromo-1,2,3-trimethoxybenzene (0.49 g, 2.0 mmol) in anhydrous THF (10 mL) was cooled to -78 °C, and then added $n\text{-BuLi}$ (2.5 M, 0.80 mL, 2.0 mmol) in drop wise via syringe. The mixture was stirred for 0.5 h at the same temperature and followed by the addition of the solution of indolone **9** (0.34 g, 1.0 mmol) in THF (20 mL). The reaction mixture was stirred at -78 °C overnight. The reaction was carefully quenched by saturated aqueous NH_4Cl and was stirred at room temperature for another 2 h. The organic layers were separated and washed with water and brine respectively, dried over Na_2SO_4 , filtered, concentrated under reduced pressure. The crude product was chromatographed on silica gel (petroleum/ethyl acetate, 3:1 as an eluent) to afford the product (0.55 g, 1.1 mmol) as yellow oil. Yield: 54%. ^1H NMR (400 MHz, Chloroform- d) δ 7.93 – 7.88

(m, 2H), 7.81 (d, $J = 8.9$ Hz, 1H), 7.58 (d, $J = 3.8$ Hz, 1H), 7.56 – 7.50 (m, 2H), 7.45 (t, $J = 7.7$ Hz, 2H), 6.77 (d, $J = 3.8$ Hz, 1H), 6.45 (s, 2H), 3.85 (s, 3H), 3.69 (s, 6H), 3.10 (dd, $J = 15.1, 6.7$ Hz, 1H), 2.79 – 2.68 (m, 1H), 2.57 (ddd, $J = 14.1, 7.2, 2.8$ Hz, 1H), 2.37 (s, 1H), 2.18 (ddd, $J = 13.8, 10.3, 3.1$ Hz, 1H), 1.94 (dt, $J = 14.5, 7.2$ Hz, 1H), 1.85 – 1.73 (m, 2H), 1.65 – 1.56 (m, 1H).

Synthesis of 3-(phenylsulfonyl)-6-(3,4,5-trimethoxyphenyl)-3,8,9,10-tetrahydrocyclo-hepta[e] indole (11)[20]

Indolol **10** (0.20 g, 0.39 mmol) and p-toluenesulfonic acid (6.7 mg, 0.039 mmol) were added in CHCl_3 (5.0 mL) at room temperature for 30 min. The reaction was quenched by saturated aqueous NaHCO_3 , and extracted with CH_2Cl_2 . The combined organic layers were washed with saturated aqueous NaCl , dried over Na_2SO_4 , filtered and concentrated under reduced pressure. The crude product was chromatographed on silica gel (8:1 of petroleum/ethyl acetate as an eluent) to afford the product (0.17g, 0.35 mmol) as white solid in 90% yield. ^1H NMR (400 MHz, Chloroform- d) δ 7.97 – 7.86 (m, 2H), 7.80 (d, $J = 8.6$ Hz, 1H), 7.61 (d, $J = 3.7$ Hz, 1H), 7.59 – 7.51 (m, 1H), 7.46 (td, $J = 7.1, 1.6$ Hz, 2H), 7.00 (d, $J = 8.6$ Hz, 1H), 6.80 (dd, $J = 3.7, 0.6$ Hz, 1H), 6.44 (d, $J = 3.0$ Hz, 3H), 3.86 (s, 3H), 3.76 (s, 6H), 2.84 (t, $J = 7.0$ Hz, 2H), 2.23 (q, $J = 7.1$ Hz, 2H), 1.92 (q, $J = 7.2$ Hz, 2H).

Synthesis of 6-(3,4,5-trimethoxyphenyl)-3,8,9,10-tetrahydrocyclohepta[e]indole (12)[35]

To a stirred suspension of cyclohepta-indole derivatives **11** (0.49 g, 1.0 mmol) in methanol (5.0 mL), 1 M KOH (aq) (1.2 mL, 1.2 mmol) was added and the mixture was stirred at refluxed for 1 h. The reaction was quenched by water, and extracted with ethyl acetate. The organic layer was collected and dried over anhydrous MgSO_4 and concentrated in vacuo to yield colorless oil. The residue was purified by flash column chromatography over silica gel (petroleum/ethyl acetate = 2:1) to afford **8** (0.28 g, 0.81 mmol) as colorless oil. Yield: 81%; ^1H NMR (400 MHz, DMSO) δ 11.10 (s, 1H), 7.34 (d, $J = 3.1$ Hz, 1H), 7.22 (d, $J = 8.4$ Hz, 1H), 6.69 (d, $J = 8.4$ Hz, 1H), 6.57 (dd, $J = 3.0, 0.6$ Hz, 1H), 6.50 (s, 2H), 6.44 (t, $J = 7.3$ Hz, 1H), 3.68 (s, 6H), 3.67 (s, 3H), 2.86 (t, $J = 6.9$ Hz, 2H), 2.27 – 2.15 (m, 2H), 1.88 (q, $J = 7.1$ Hz, 2H).

^{13}C NMR (101 MHz, CDCl_3) δ 152.84, 144.01, 139.09, 137.13, 134.80, 134.57, 130.82, 127.30, 127.03, 124.16, 124.04, 108.51, 105.29, 101.14, 60.98, 56.13, 35.78, 28.18, 25.91. HRMS (ESI) (m/z) $[\text{M}+\text{Na}]^+$ calcd. for $\text{C}_{22}\text{H}_{23}\text{N O}_3$, 350.1751; found, 350.1751. Purity: 98.5% (by HPLC).

General procedure for the preparation of **13**[34]

To a solution of **12** (0.35 g, 1.0 mmol) in anhydrous THF, NaH (1.2 mmol) was added at 0 °C. After the mixture was stirred for 15 minutes, a corresponding iodohydrocarbon or bromohydrocarbon (1.0 mmol) in THF was added in drop wise. The mixture was stirred at room temperature for 4 h. The organic layer was washed with brine and then dried (Na_2SO_4). The solvents were removed under reduced pressure to obtain the crude product, which was purified by silica gel column chromatography (petroleum ether/ ethyl acetate =4:1) to provide **13**.

3-methyl-6-(3,4,5-trimethoxyphenyl)-3,8,9,10-tetrahydrocyclohepta[e]indole

(**13a**)

Colorless oil. (0.31 g, 0.85 mmol) Yield 85%. ^1H NMR (400 MHz, Chloroform-*d*) δ 7.15 (d, $J = 8.5$ Hz, 1H), 7.09 (d, $J = 3.1$ Hz, 1H), 6.93 (d, $J = 8.5$ Hz, 1H), 6.63 – 6.60 (m, 1H), 6.53 (s, 2H), 6.45 (t, $J = 7.3$ Hz, 1H), 3.87 (s, 3H), 3.81 (s, 3H), 3.78 (s, 6H), 2.96 (t, $J = 7.0$ Hz, 2H), 2.30 (p, $J = 7.1$ Hz, 2H), 1.98 (q, $J = 7.2$ Hz, 2H). ^{13}C NMR (101 MHz, CDCl_3) δ 152.83, 143.98, 138.97, 137.22, 135.68, 134.71, 130.41, 128.49, 127.50, 127.12, 123.79, 106.63, 105.28, 99.49, 60.92, 56.12, 35.70, 32.99, 28.04, 25.87. HRMS (ESI) (m/z) $[\text{M}+\text{Na}]^+$ calcd. for $\text{C}_{23}\text{H}_{25}\text{N O}_3$, 364.1907; found, 364.1912. Purity: 95.1% (by HPLC).

3-ethyl-6-(3,4,5-trimethoxyphenyl)-3,8,9,10-tetrahydrocyclohepta[e]indole (**13b**)

Colorless oil. (0.33 g, 0.87 mmol) Yield 87%. ^1H NMR (400 MHz, Chloroform-*d*) δ 7.20 – 7.14 (m, 2H), 6.91 (d, $J = 8.5$ Hz, 1H), 6.62 (d, $J = 3.1$ Hz, 1H), 6.54 (s, 2H), 6.44 (t, $J = 7.3$ Hz, 1H), 4.18 (q, $J = 7.3$ Hz, 2H), 3.86 (s, 3H), 3.78 (s, 6H), 2.96 (t, $J = 7.0$ Hz, 2H), 2.37 – 2.25 (m, 2H), 1.98 (q, $J = 7.2$ Hz, 2H), 1.50 (t, $J = 7.3$ Hz, 3H). ^{13}C NMR (101 MHz, CDCl_3) δ 152.82, 144.03, 139.04, 137.19, 134.83, 134.73, 130.38, 127.62, 127.19, 126.67, 123.66, 106.72, 105.31, 99.58, 60.93, 56.15, 41.11,

35.75, 28.09, 25.91, 15.52. HRMS (ESI) (m/z) [M+Na]⁺ calcd. for C₂₄H₂₇N O₃, 378.2064; found, 378.2067. Purity: 96.3% (by HPLC).

3-propyl-6-(3,4,5-trimethoxyphenyl)-3,8,9,10-tetrahydrocyclohepta[e]indole (13c)

Colorless oil. (0.35 g, 0.90 mmol) Yield 90%. ¹H NMR (400 MHz, Chloroform-d) δ 7.15 (d, *J* = 10.4 Hz, 2H), 6.89 (d, *J* = 8.5 Hz, 1H), 6.60 (s, 1H), 6.54 (s, 2H), 6.43 (t, *J* = 7.2 Hz, 1H), 4.07 (t, *J* = 7.0 Hz, 2H), 3.86 (s, 3H), 3.78 (d, *J* = 2.1 Hz, 6H), 2.96 (t, *J* = 6.8 Hz, 2H), 2.30 (p, *J* = 6.4 Hz, 2H), 1.98 (q, *J* = 6.9 Hz, 2H), 1.88 (dt, *J* = 13.0, 6.6 Hz, 2H), 0.98 (td, *J* = 7.5, 2.1 Hz, 3H). ¹³C NMR (101 MHz, CDCl₃) δ 152.83, 144.05, 139.05, 137.27, 135.05, 134.76, 130.32, 127.60, 127.54, 127.14, 123.61, 106.82, 105.39, 99.39, 60.92, 56.16, 48.27, 35.74, 28.10, 25.92, 23.61, 11.64. HRMS (ESI) (m/z) [M+Na]⁺ calcd. for C₂₅H₂₉N O₃, 392.2220; found, 392.2237. Purity: 96.2% (by HPLC).

Synthesis

of

6-(3,4,5-trimethoxyphenyl)-1,2,3,8,9,10-hexahydrocyclohepta[e]indole (14)[42]

To a stirred solution of cyclohepta-indole derivatives **12** (0.17 g, 0.5 mmol) in AcOH (10 mL), NaBH₃CN (94 mg, 1.5 mmol) was added. After the mixture was further stirred for 4.0 h under N₂, the reaction was quenched by adding of water. The solvent was removed in vacuo and the product was extracted with ethyl acetate. The organic layer was washed with saturated aqueous NaHCO₃, dried with Na₂SO₄ and concentrated under reduced pressure to give crude product as colourless oil. The crude product was purified by silica gel column chromatography (petroleum ether/ ethyl acetate =2:1) to provide **14** (0.13 g, 0.36 mmol) as colorless oil. Yield: 71%. ¹H NMR (400 MHz, Chloroform-d) δ 6.73 (d, *J* = 8.0 Hz, 1H), 6.52 (s, 2H), 6.48 (d, *J* = 8.0 Hz, 1H), 6.26 (t, *J* = 7.3 Hz, 1H), 3.85 (s, 3H), 3.80 (s, 6H), 3.63 (t, *J* = 8.4 Hz, 2H), 3.09 (t, *J* = 8.4 Hz, 2H), 2.57 (t, *J* = 6.9 Hz, 2H), 2.13 (p, *J* = 7.1 Hz, 2H), 1.98 (q, *J* = 7.1 Hz, 2H). ¹³C NMR (101 MHz, CDCl₃) δ 152.78, 150.27, 143.49, 138.92, 138.29, 130.98, 128.99, 128.10, 126.68, 125.84, 106.78, 105.45, 60.88, 56.15, 47.13, 33.96, 28.75, 28.52, 25.76. HRMS (ESI) (m/z) [M+Na]⁺ calcd. for C₂₂H₂₅N O₃, 352.1907; found, 352.1907. Purity: 97.2% (by HPLC).

Synthesis **of**
3-methyl-6-(3,4,5-trimethoxyphenyl)-1,2,3,8,9,10-hexahydrocyclohepta[e]indole
(15)[34]

To a solution of **14** (0.18 g, 0.50 mmol) in anhydrous THF, NaH (24 mg, 0.60 mmol, 60 %) was added. After the mixture was stirred for 15 minutes, iodomethane (63 μ L, 1.0 mmol) in THF was added in dropwise. The mixture was stirred at room temperature. Organic layer was washed with brine and dried. The solvents were removed under reduced pressure to obtain the crude product, which was purified by silica gel column chromatography (petroleum ether/ ethyl acetate =4:1) to provide indoline **15** (0.17 g, 0.46 mmol) as colorless oil. Yield 91%. ¹H NMR (400 MHz, Chloroform-d) δ 6.79 (d, J = 8.0 Hz, 1H), 6.53 (s, 2H), 6.33 (d, J = 8.1 Hz, 1H), 6.24 (t, J = 7.2 Hz, 1H), 3.86 (s, 3H), 3.80 (s, 6H), 3.39 (t, J = 8.2 Hz, 2H), 3.00 (t, J = 8.2 Hz, 2H), 2.79 (s, 3H), 2.56 (t, J = 6.9 Hz, 2H), 2.12 (d, J = 7.0 Hz, 2H), 1.98 (q, J = 7.0 Hz, 2H). ¹³C NMR (101 MHz, CDCl₃) δ 152.77, 152.06, 143.49, 139.06, 137.86, 137.24, 130.21, 129.16, 127.33, 125.67, 105.41, 104.52, 60.91, 56.16, 55.86, 36.17, 33.82, 29.71, 28.32, 27.54, 25.79. HRMS (ESI) (m/z) [M+Na]⁺ calcd. for C₂₃H₂₇N O₃, 366.2064; found, 366.2068. Purity: 99.1% (by HPLC).

Synthesis **of**
6-(3,4,5-trimethoxyphenyl)-3,8,9,10-tetrahydrocyclohepta[e]indole-1-carbaldehyde
(16)[43]

To a stirred solution of indole derivatives **12** (0.17 g, 0.5 mmol) in AcOH (5.0 mL), hexamethylenetetramine (0.11 g, 0.75 mol) was added at room temperature. After heated at reflux under N₂ for 18 h, the mixture was diluted with water (10 mL), neutralized with saturated aqueous NaHCO₃ until no CO₂ was evolved. The mixture was extracted with ethyl acetate, and the organic layer was washed with water, brine and dried over Na₂SO₄. After removal of solvent by evaporation, the crude product was obtained as an orange oil, which was purified by silica gel chromatography eluted with petroleum ether/ ethyl acetate =1: 1 to give **16** (0.11 g, 0.29 mmol) as yellow solid. Yield: 58%. ¹H NMR (400 MHz, Chloroform-d) δ 10.09 (s, 1H), 9.02 (s, 1H), 7.96 (d, J = 3.2 Hz, 1H), 7.23 (d, J = 8.4 Hz, 1H), 7.02 (d, J = 8.4 Hz, 1H), 6.53 (d, J

= 9.0 Hz, 3H), 3.87 (s, 3H), 3.79 (s, 6H), 3.38 (t, $J = 6.9$ Hz, 2H), 2.39 (p, $J = 7.1$ Hz, 2H), 1.96 (q, $J = 7.2$ Hz, 2H). ^{13}C NMR (101 MHz, CDCl_3) δ 191.16, 184.34, 152.89, 143.26, 138.93, 138.25, 137.15, 136.78, 135.41, 128.92, 126.22, 123.47, 121.12, 109.13, 105.30, 60.99, 56.13, 36.72, 29.72, 25.66. HRMS (ESI) (m/z) $[\text{M}+\text{Na}]^+$ calcd. for $\text{C}_{23}\text{H}_{23}\text{NO}_4$, 378.1700; found, 378.1697. Purity: 97.7% (by HPLC).

Synthesis of
3-methyl-6-(3,4,5-trimethoxyphenyl)-3,8,9,10-tetrahydrocyclohepta[e] indole-1-carbaldehyde (17)[43]

To a stirred solution of **13a** (0.18 g, 0.50 mmol) in AcOH (5.0 mL), hexamethylenetetramine (0.11 g, 0.75 mmol) was added at room temperature. The mixture was heated to reflux under N_2 for 18 h, and then, diluted with water (10 mL), neutralized with saturated aqueous NaHCO_3 until no CO_2 was evolved. The mixture was extracted with ethyl acetate, organic layer was washed with water, brine and dried over Na_2SO_4 . After removal of solvent by evaporation, aldehyde **17** (0.12 g, 0.31 mmol) was obtained as yellow oil. Yield: 61%. ^1H NMR (400 MHz, Chloroform- d) δ 10.04 (s, 1H), 7.81 (s, 1H), 7.18 (d, $J = 8.5$ Hz, 1H), 7.07 (d, $J = 8.5$ Hz, 1H), 6.52 (d, $J = 3.7$ Hz, 3H), 3.88 (d, $J = 3.7$ Hz, 6H), 3.79 (s, 6H), 3.38 (t, $J = 6.9$ Hz, 2H), 2.38 (p, $J = 7.0$ Hz, 2H), 1.95 (q, $J = 7.2$ Hz, 2H). ^{13}C NMR (101 MHz, CDCl_3) δ 183.64, 152.94, 143.22, 141.66, 138.75, 137.83, 137.32, 135.42, 128.86, 125.90, 124.27, 119.49, 107.35, 105.29, 60.96, 56.14, 36.59, 33.85, 30.23, 25.64. HRMS (ESI) (m/z) $[\text{M}+\text{Na}]^+$ calcd. for $\text{C}_{24}\text{H}_{25}\text{NO}_4$, 392.1856; found, 392.1865. Purity: 95.1% (by HPLC).

Synthesis of
(3-methyl-6-(3,4,5-trimethoxyphenyl)-3,8,9,10-tetrahydrocyclohepta[e]indol-1-yl) methanol (18)[44]

To a stirred solution of aldehyde **17** (0.20 g, 0.50 mmol) in CH_3OH (10 mL), NaBH_4 (57 mg, 1.5 mmol) was added in portions at 10 – 15 °C. After stirred at room temperature for 3 h, the mixture was quenched by addition of 5.0 mL of H_2O , extracted by ethyl acetate, washed with brine dried with NaSO_4 and concentration under reduced pressure to obtain the crude product. The crude product was purified by

silica gel column chromatography (petroleum ether/ ethyl acetate =4:1) to provide **19** (0.17 g, 0.42 mmol) as colorless oil. Yield: 83%. ¹H NMR (400 MHz, Chloroform-d) δ 7.12 (d, *J* = 8.5 Hz, 1H), 7.09 (s, 1H), 6.95 (d, *J* = 8.5 Hz, 1H), 6.54 (s, 2H), 6.46 (t, *J* = 7.3 Hz, 1H), 4.94 (s, 2H), 3.87 (s, 3H), 3.78 (s, 6H), 3.76 (s, 3H), 3.12 (t, *J* = 6.8 Hz, 2H), 2.33 (p, *J* = 6.9 Hz, 2H), 1.95 (q, *J* = 7.1 Hz, 2H). ¹³C NMR (101 MHz, CDCl₃) δ 152.87, 143.79, 138.97, 137.32, 137.08, 135.32, 131.92, 129.15, 127.42, 124.76, 124.30, 114.94, 106.77, 105.40, 60.92, 58.51, 56.17, 36.59, 32.79, 27.82, 25.66. HRMS (ESI) (*m/z*) [M+Na]⁺ calcd. for C₂₄ H₂₇ N O₄, 416.1832; found, 416.1818. Purity: 95.5 % (by HPLC).

Synthesis of methyl 2-(3-methyl-6-(3,4,5-trimethoxyphenyl)-3,8,9,10-tetrahydrocyclohepta[e]indol-1-yl)-2-oxoacetate (19)[45]

To a solution of **13a** (0.18 g, 0.50 mmol) in Et₂O (5.0 mL) at 0 °C, oxalyl chloride (48 μL, 0.55 mmol) was added. The resulting yellow slurry was stirred at 0 °C for 1.5 h and then at room temperature for 1.5 h. The organic solvent was removed under reduced pressure to get yellow solid. The residue was cooled to 0 °C, the, CH₃OH (5.0 mL) and Et₃N (2.0 mL) were added. The mixture was stirred at 0 °C for 1 h and then warmed to room temperature over 4 h. The mixture was extracted with ethyl acetate and the organic layer was washed with water, brine and dried over Na₂SO₄. The organic layer was evaporated to dryness to provide yellow oil. The crude product was purified by silica gel column chromatography (petroleum ether/ ethyl acetate =4:1) to provide **19** (0.16 g, 0.37 mmol) as flaxen oil. Yield: 73%. ¹H NMR (400 MHz, Chloroform-d) δ 8.23 (s, 1H), 7.18 (d, *J* = 8.5 Hz, 1H), 7.09 (d, *J* = 8.5 Hz, 1H), 6.54 (d, *J* = 7.3 Hz, 1H), 6.50 (s, 2H), 3.96 (s, 3H), 3.86 (d, *J* = 3.0 Hz, 6H), 3.78 (s, 6H), 3.29 (t, *J* = 6.3 Hz, 2H), 2.47 (p, *J* = 6.6 Hz, 2H), 1.96 (q, *J* = 7.1 Hz, 2H). ¹³C NMR (101 MHz, CDCl₃) δ 177.72, 165.10, 152.93, 143.11, 142.40, 138.93, 138.16, 137.55, 137.37, 136.55, 129.42, 126.55, 125.25, 113.82, 107.29, 105.40, 60.90, 56.14, 52.69, 37.34, 33.95, 30.25, 25.66. HRMS (ESI) (*m/z*) [M+Na]⁺ calcd. for C₂₆ H₂₇ N O₆, 450.1911; found, 450.1929. Purity: 97.5% (by HPLC).

Synthesis

of

3-methyl-6-(3,4,5-trimethoxyphenyl)-3,6,7,8,9,10-hexahydrocyclohepta[e]indole (20)[46]

To a stirred suspension of **13a** (0.18 g, 0.50 mmol) in methanol (5.0 mL), Pd/C (50 mg) was added and the mixture was stirred under H₂ balloon at room temperature for 3 h. Then, filtered and vacuumed to get the crude product which was purified by silica gel column chromatography (petroleum ether/ ethyl acetate = 4:1) to provide the title compound (0.16 g, 0.45 mmol). Yield: 89%. ¹H NMR (400 MHz, Chloroform-d) δ 7.06 (d, *J* = 3.2 Hz, 1H), 7.02 (d, *J* = 8.5 Hz, 1H), 6.66 (d, *J* = 8.5 Hz, 1H), 6.55 (d, *J* = 3.1 Hz, 1H), 6.50 (s, 2H), 4.39 (d, *J* = 8.3 Hz, 1H), 3.90 (s, 3H), 3.83 (d, *J* = 4.6 Hz, 7H), 3.77 (s, 3H), 3.22 (dd, *J* = 13.2, 7.5 Hz, 1H), 3.17 – 3.05 (m, 1H), 2.29 – 2.18 (m, 1H), 2.16 – 1.83 (m, 5H). ¹³C NMR (101 MHz, CDCl₃) δ 153.07, 141.75, 136.01, 135.45, 134.23, 128.53, 128.47, 122.88, 106.14, 105.69, 99.98, 99.32, 60.94, 56.10, 49.67, 34.34, 32.89, 30.61, 30.19, 27.08. HRMS (ESI) (*m/z*) [*M*+Na]⁺ calcd. for C₂₃H₂₇NO₃, 366.2064; found, 366.2068. Purity: 99.3 % (by HPLC).

Synthesis of (E)-3-(1-(phenylsulfonyl)-1H-indol-4-yl)acrylic acid (21)[47]

To a stirred suspension of aldehyde **6** (1.0 g, 3.5 mmol) in pyridine (40 mL), malonic acid (0.73 g, 7.0 mmol) and piperidine (1.0 mL) were added and the mixture was heated to reflux at 120 °C for 3 h. When allowed to cool to 0 °C, the mixture was acidified by hydrochloric acid. The precipitate was filtered and the filter cake was washed with 20 mL of H₂O, dried in vacuum to afford the crude product which was purified by re-crystallization from a mixed-solvent (ethyl acetate: methanol = 4 : 1) to give a white solid (0.89 g, 2.7 mmol). Yield: 78%. ¹H NMR (400 MHz, DMSO-d₆) δ 8.07 – 7.99 (m, 4H), 7.95 (d, *J* = 3.8 Hz, 1H), 7.89 (d, *J* = 16.1 Hz, 1H), 7.70 (d, *J* = 7.4 Hz, 2H), 7.61 (dd, *J* = 8.5, 7.1 Hz, 2H), 7.42 (d, *J* = 8.0 Hz, 1H), 7.21 (d, *J* = 3.8 Hz, 1H), 6.62 (d, *J* = 16.0 Hz, 1H).

Synthesis of 3-(1-(phenylsulfonyl)-1H-indol-4-yl)propanoic acid (22)[35]

To a stirred suspension of acrylic acid **21** (0.98 g, 3.0 mmol) in methanol (10 mL), Pd/C (0.15 g) was added and the mixture was stirred under H₂ balloon at room temperature for 3 h. Then, the mixture was filtered and vacuumed to get colorless oil.

The crude product was used directly for the next step without purification. (0.47 g, 1.4 mmol) Yield: 48%. ^1H NMR (400 MHz, DMSO- d_6) δ 8.02 – 7.95 (m, 2H), 7.82 (d, J = 3.8 Hz, 1H), 7.80 (d, J = 8.4 Hz, 1H), 7.72 – 7.66 (m, 1H), 7.59 (t, J = 7.7 Hz, 2H), 7.31 – 7.23 (m, 1H), 7.10 (d, J = 7.3 Hz, 1H), 7.00 – 6.94 (m, 1H), 3.03 (t, J = 7.6 Hz, 2H), 2.56 (t, J = 7.7 Hz, 2H).

Synthesis of 3-(phenylsulfonyl)-7,8-dihydrocyclopenta[e]indol-6(3H)-one (**23**)[41]

Propanoic acid **22** (1.0 g, 2.8 mmol) was added in small portions to 10 g of rapidly stirred solution of phosphorus pentoxide:methanesulfonic acid (1:10). After the reaction mixture was stirred at room temperature for 4 h, 40 ml of water was added in dropwise and the aqueous mixture was stirred rapidly for 5-10 min to ensure the hydrolysis of methanesulfonic anhydride. The mixture was extracted with ethyl acetate, washed subsequently with dilute sodium bicarbonate and water, dried over anhydrous sodium sulfate, and concentrated in vacuum. The crude product was chromatographed on silica gel (4:1 of petroleum/ethyl acetate as an eluent) to afford the product (0.42g, 1.3 mmol) as white solid in 48% yield. ^1H NMR (400 MHz, Chloroform- d) δ 8.02 (d, J = 8.6 Hz, 1H), 7.91 (d, J = 8.0 Hz, 2H), 7.75 – 7.67 (m, 2H), 7.57 (t, J = 7.4 Hz, 1H), 7.48 (t, J = 7.6 Hz, 2H), 6.82 (t, J = 2.8 Hz, 1H), 3.24 (t, J = 4.9 Hz, 2H), 2.83 – 2.70 (m, 2H).

Synthesis of 7,8-dihydrocyclopenta[e]indol-6(3H)-one (**24**)[35]

To a stirred suspension of indolone derivatives **23** (0.31 g, 1.0 mmol) in methanol (5.0 mL), 1 M KOH (aq) (1.2 mL, 1.2 mmol) was added. The mixture was stirred at reflux for 2 h. The reaction was quenched by water, and extracted with ethyl acetate. The organic layer was collected and dried over anhydrous MgSO_4 , concentrated in vacuo to yield colorless oil. The residue was purified by flash column chromatography over silica gel (petroleum/ethyl acetate = 1:1) to afford **24** (0.14 g, 0.81 mmol). Yield: 81%; ^1H NMR (400 MHz, Chloroform- d) δ 8.69 (s, 1H), 7.61 (d, J = 8.5 Hz, 1H), 7.39 (dq, J = 8.5, 0.8 Hz, 1H), 7.33 (dd, J = 3.3, 2.4 Hz, 1H), 6.73 (ddd, J = 3.1, 2.0, 1.0 Hz, 1H), 3.41 – 3.25 (m, 2H), 2.84 – 2.72 (m, 2H).

Synthesis of 3-methyl-7,8-dihydrocyclopenta[e]indol-6(3H)-one (**25**)[34]

To a solution of **24** (0.37 g, 2.0 mmol) in anhydrous THF, NaH (80mg, 2.0 mmol,

60%) was added at 0 °C. After the mixture was stirred for 15 minutes, a corresponding iodohydrocarbon (0.11 mL, 2.0 mmol) in THF was added in dropwise. The mixture was stirred at room temperature for 4 h. Organic layer wash with brine and dried. The solvents were removed under reduced pressure to obtain the crude product, which was purified by silica gel column chromatography (petroleum ether/ethyl acetate =8:1) to provide **25** (0.34 g, 1.8 mmol) as colorless oil. Yield 91%. ¹H NMR (400 MHz, Chloroform-*d*) δ 7.62 (dd, *J* = 8.5, 1.8 Hz, 1H), 7.34 – 7.28 (m, 1H), 7.16 (t, *J* = 2.5 Hz, 1H), 6.65 (t, *J* = 2.4 Hz, 1H), 3.87 (s, 3H), 3.33 – 3.24 (m, 2H), 2.82 – 2.71 (m, 2H).

Synthesis of 3-methyl-6-(3,4,5-trimethoxyphenyl)-3,8-dihydrocyclopenta[*e*]indole (**26**)[20]

To a solution of 5-bromo-1,2,3-trimethoxybenzene (0.49 g, 2.0 mmol) in anhydrous THF (10 mL) at –78 °C under the argon atmosphere, *n*-BuLi (2.5 M, 0.80 mL, 2.0 mmol) was added in dropwise via a syringe. The mixture was stirred for 0.5 h at the same temperature and followed by addition of the solution of **21** (0.19 g, 1.0 mmol) in THF (10 mL). The reaction mixture was stirred for 1 hour at –78 °C then allowed to warm to room temperature. After stirred for another 2 h, the reaction was carefully quenched by saturated aqueous NH₄Cl and extracted with ethyl acetate. The combined organic layers were and washed with water and brine respectively, dried over Na₂SO₄, filtered and concentrated under reduced pressure. The crude product was chromatographed on silica gel and eluted with petroleum/ethyl acetate (4:1) to afford the **26** (0.36g, 1.1 mmol) as a yellow oil. Yield: 54% ¹H NMR (400 MHz, Chloroform-*d*) δ 7.49 (d, *J* = 8.4 Hz, 1H), 7.26 (d, *J* = 8.4 Hz, 1H), 7.07 (d, *J* = 3.1 Hz, 1H), 6.88 (s, 2H), 6.53 (dd, *J* = 3.1, 0.8 Hz, 1H), 6.42 (t, *J* = 2.1 Hz, 1H), 3.91 (s, 3H), 3.90 (s, 6H), 3.77 (s, 3H), 3.64 (d, *J* = 2.1 Hz, 2H). ¹³C NMR (101 MHz, CDCl₃) δ 153.34, 145.97, 137.45, 137.21, 135.83, 135.68, 132.87, 129.69, 126.90, 125.73, 114.62, 107.34, 104.97, 98.77, 61.02, 56.21, 37.03, 33.19. HRMS (ESI) (*m/z*) [M+Na]⁺ calcd. for C₂₁ H₂₁ N O₃, 336.1594; found, 336.1599. Purity: 98.2% (by HPLC).

4.2 Biological assays

4.2.1 Cell lines and culture

Seven types of human cancer cell lines used in this study were obtained from the Laboratory Animal Center of Sun Yat-sen University. The non-small cell lung cancer cell line A549, human epithelial cervical cancer cell line HeLa, human prostate cancer line PC-3, human liver carcinoma cell line Bel-7402, human colon cancer cell line Lovo, human ovarian cancer cell line A2780, and human breast carcinoma cell line MCF-7 were grown in Dulbecco's modified Eagle medium (DMEM, GIBCO) containing 10% (v/v) heat-inactivated fetal bovine serum (FBS, GIBCO), 100 IU/mL penicillin, and 100 µg/mL streptomycin (GIBCO). The cells were incubated at 37 °C in a 5% CO₂ and 90% relative humidity (RH) atmosphere.

4.2.2 *In vitro* antiproliferative activity assays

The antiproliferative activities of the synthesized compounds towards seven human cancer cell lines (A549, HeLa, PC-3, Bel-7402, Lovo, A2780, and MCF-7) were evaluated using the MTT assay as previously described. [24] Briefly, when growing in the logarithmic phase, the cells were harvested and plated into 96-well plates (5×10^3 cells/well) for 24 h and then exposed to different concentrations of the test compounds for 48 h. Subsequently, 20 µL of MTT (5 mg/mL, Sigma) and 150 µL of DMSO were added to dissolve the dark blue crystals (formazan). The absorbance at 570 nm was measured using a multifunction microplate reader (Molecular Devices, Flex Station 3). The antiproliferative activities of the optimized compound **20** were also determined by the CCK-8 assay. Briefly, after treatment, 10 µl CCK-8 solution (Keygen Biotech, Nanjin, China) were added to each well and incubated for 2 h. The absorbance at 450 nm was measured. All experiments were repeated at least three times. The IC₅₀ values, which represent the drug concentrations required to cause 50% tumour cell growth inhibition, were calculated using a nonlinear regression model (GraphPad Prism version 5.0).

4.2.3 *In vitro* tubulin polymerization inhibition

The tubulin polymerization assay was performed as previously described [22]

using a commercial kit (cytoskeleton, cat.#BK011P) purchased from Cytoskeleton (Danvers, MA, USA). Tubulin isolated from porcine brain tissue was used in this tubulin polymerization assay kit. Tubulin polymerizations are followed by an increase in fluorescence emission at 410-460 nm over a 60 minute period at 37 °C. Firstly, the tubulin reaction mix containing 80.0 mM piperazine-N, N'-bis(2-ethanesulfonic acid) sequisodium salt (pH 6.9), 2.0 mM MgCl₂, 0.5 mM EGTA, 1 mM GTP, and 10.2% glycerol was prepared. Then, 5 μL of the tested compounds at the indicated concentrations were added, and the mixture was pre-warmed to 37 °C for 1 min. Subsequently, the reaction was initiated by the addition of 55 μL tubulin solution. The fluorescence intensity was recorded every 60 sec for 90 min in a multifunction microplate reader (Molecular Devices, Flex Station 3) (emission wavelength is 410 nm, excitation wavelength is 340 nm). The area under the curve was used to determine the concentration that inhibited tubulin polymerization by 50% (IC₅₀), which was calculated with GraphPad Prism Software version 5.02 (GraphPad Inc., La Jolla, CA, USA).

4.2.4 Immunofluorescence microscopy.

The intracellular microtubule morphology was detected using immunofluorescence as previously described. [22] Briefly, A549 cells (3×10^5 cells/well) were plated in a 10 mm³ confocal culture dish (NEST Biotechnology, China) for 24 h and then incubated in the presence or absence of compound **20** at the indicated concentrations for another 12 h. After being washed with phosphate buffer solution (PBS) and fixed in 4% paraformaldehyde for 15 min, the cells were permeabilized with 0.5% Triton X-100

for 15 min and blocked for 30 min with 10% goat serum. Then, the cells were incubated with mouse anti-tubulin antibody (CST, USA) at 4 °C overnight and incubated with goat anti-mouse IgG/Alexa-Fluor 488 antibody (Invitrogen, USA) at room temperature for 1 h. After the nuclei were stained with Hoechst 33342 (Sigma, USA) in the dark at room temperature for 30 min, the samples were immediately visualized on a Zeiss LSM 570 laser scanning confocal microscope (Carl Zeiss, Germany).

4.2.5 Cell cycle analysis.

For the flow cytometric analysis of the DNA content, A549 cells were seeded in 6-well plates (3×10^5 cells/well) and incubated in the presence or absence of compound **20** at indicated concentrations for 24 or 48 h. After treatment, cells were detached with 0.25% trypsin, harvested by centrifugation, and then fixed in 70% ethanol at 4 °C overnight. Ethanol was removed by centrifugation, and the cells were re-suspended in ice-cold PBS and treated with RNase A (Keygen Biotech, China) at 37 °C for 30 min, followed by incubation with the DNA staining solution propidium iodide (PI) (Keygen Biotech, China) at 4 °C for 30 min. The DNA content of 10,000 events was analysed using a flow cytometer (Beckman Coulter, Epics XL) at 488 nm. The data regarding the number of cells in different phases of the cell cycle were analysed using the EXPO32 ADC analysis software.

4.2.6 Apoptosis analysis.

For apoptosis analysis, the sample preparation process was the same as described for the cell cycle analysis. After harvesting by centrifugation, the cells were incubated with 5 µL of Annexin-V/FITC (Keygen Biotech, China) in binding buffer (10 mM HEPES, 140 mM NaCl, and 2.5 mM CaCl₂ at pH 7.4) at room temperature for 15 min

and then PI solution (Keygen Biotech, China) for another 10 min-incubation. Almost 10,000 events were collected for each sample and analysed by flow cytometry (Beckman Coulter, Epics XL). The percentage of apoptotic cells was calculated using the EXPO32 ADC analysis software.

SUPPORTING INFORMATION

HPLC chromatograms, NMR spectra and high resolution mass spectra of target compounds and some supplementary figures of biological activity.

ACKNOWLEDGMENT

This work was supported by the National Natural Science Foundation of China (No. 21302235, 20972198), Guangdong Natural Science Foundation (2014A030313124) and the Fundamental Research Funds for the Central Universities (15ykpy04).

References

- [1] K.H. Downing, E. Nogales, Tubulin and microtubule structure, *Curr. Opin. Cell Biol.* 10 (1998) 16-22.
- [2] F. Pellegrini, D.R. Budman, Review: Tubulin function, action of antitubulin drugs, and new drug development, *Cancer Invest.* 23 (2005) 264-273.
- [3] R.A. Walker, E.T. O'Brien, N.K. Pryer, M.F. Soboeiro, W.A. Voter, H.P. Erickson, E.D. Salmon, Dynamic instability of individual microtubules analyzed by video light microscopy: rate constants and transition frequencies, *J. Cell Biol.* 107 (1988) 1437-1448.
- [4] S. Honore, E. Pasquier, D. Braguer, Understanding microtubule dynamics for improved cancer therapy, *Cell. Mol. Life Sci.* 62 (2005) 3039-3056.
- [5] J.C. Zabala, N.J. Cowan, Tubulin dimer formation via the release of alpha- and beta-tubulin monomers from multimolecular complexes, *Cell. Motil. Cytoskeleton* 23 (1992) 222-230.
- [6] K.H. Downing, E. Nogales, Tubulin structure: insights into microtubule properties and functions, *Curr. Opin. Struct. Biol.* 8 (1998) 785-791.

- [7] M.A. Jordan, L. Wilson, Microtubules as a target for anticancer drugs, *Nat. Rev. Cancer* 4 (2004) 253-265.
- [8] M.A. Jordan, Mechanism of action of antitumor drugs that interact with microtubules and tubulin, *Curr. Med. Chem. Anti-Cancer Agents* 2 (2002) 1-17.
- [9] R.A. Stanton, K.M. Gernert, J.H. Nettles, R. Aneja, Drugs that target dynamic microtubules: a new molecular perspective, *Med. Res. Rev.* 31 (2011) 443-481.
- [10] H. Chen, Y. Li, C. Sheng, Z. Lv, G. Dong, T. Wang, J. Liu, M. Zhang, L. Li, T. Zhang, D. Geng, C. Niu, K. Li, Design and synthesis of cyclopropylamide analogues of combretastatin-A4 as novel microtubule-stabilizing agents, *J. Med. Chem.* 56 (2013) 685-699.
- [11] E. Boyland, M.E. Boyland, Studies in tissue metabolism: the action of colchicine and *B. typhosus* extract, *Biochem. J.* 31 (1937) 454-460.
- [12] G.R. Pettit, Singh SB, Hamel E, Lin CM, Alberts DS, Garcia-Kendall D., Isolation and structure of the strong cell growth and tubulin inhibitor combretastatin A-4, *Experientia* 45 (1989) 680.
- [13] N.H. Nam, Combretastatin A-4 analogues as antimetabolic antitumor agents, *Curr. Med. Chem.* 10 (2003) 1697-1722.
- [14] R. Kaur, G. Kaur, R.K. Gill, R. Soni, J. Bariwal, Recent developments in tubulin polymerization inhibitors: an overview, *Eur. J. Med. Chem.* 87 (2014) 89-124.
- [15] M. Marrelli, F. Conforti, G.A. Statti, X. Cachet, S. Michel, F. Tillequin, F. Menichini, Biological potential and structure-activity relationships of most recently developed vascular disrupting agents: an overview of new derivatives of natural combretastatin A-4, *Curr. Med. Chem.* 18 (2011) 3035-3081.
- [16] Y.S. Shan, J. Zhang, Z. Liu, M. Wang, Y. Dong, Developments of combretastatin A-4 derivatives as anticancer agents, *Curr. Med. Chem.* 18 (2011) 523-538.
- [17] E. Porcù, R. Bortolozzi, G. Basso, G. Viola, Recent advances in vascular disrupting agents in cancer therapy, *Future Med. Chem.* 6 (2014) 1485-1498.
- [18] R. Harish, D. Pramod Kumar, P. Vijay, J. Deepak Kumar, S. Avineesh, V. Ravichandran, S. Prabodh Chander, D. Anshuman, Design of combretastatin A-4 analogs as tubulin targeted vascular disrupting agent with special emphasis on their

- cis*-restricted isomers, *Curr. Pharm. Design*, 19 (2013) 1923-1955.
- [19] R. Mikstacka, T. Stefanski, J. Rozanski, Tubulin-interactive stilbene derivatives as anticancer agents, *Cell. Mol. Biol. Lett.* 18 (2013) 368-397.
- [20] M. Sriram, J.J. Hall, N.C. Grohmann, T.E. Strecker, T. Wootton, A. Franken, M.L. Trawick, K.G. Pinney, Design, synthesis and biological evaluation of dihydronaphthalene and benzosuberene analogs of the combretastatins as inhibitors of tubulin polymerization in cancer chemotherapy, *Bioorg. Med. Chem.* 16 (2008) 8161-8171.
- [21] R.P. Tanpure, C.S. George, T.E. Strecker, L. Devkota, J.K. Tidmore, C.M. Lin, C.A. Herdman, M.T. Macdonough, M. Sriram, D.J. Chaplin, M.L. Trawick, K.G. Pinney, Synthesis of structurally diverse benzosuberene analogues and their biological evaluation as anti-cancer agents, *Bioorg. Med. Chem.* 21 (2013) 8019-8032.
- [22] L. Devkota, C.-M. Lin, T.E. Strecker, Y. Wang, J.K. Tidmore, Z. Chen, R. Guddneppanavar, C.J. Jelinek, R. Lopez, L. Liu, E. Hamel, R.P. Mason, D.J. Chaplin, M.L. Trawick, K.G. Pinney, Design, synthesis, and biological evaluation of water-soluble amino acid prodrug conjugates derived from combretastatin, dihydronaphthalene, and benzosuberene-based parent vascular disrupting agents, *Bioorg. Med. Chem.* 24 (2016) 938-956.
- [23] R.P. Tanpure, C.S. George, M. Sriram, T.E. Strecker, J.K. Tidmore, E. Hamel, A.K. Charlton-Sevcik, D.J. Chaplin, M.L. Trawick, K.G. Pinney, An amino-benzosuberene analogue that inhibits tubulin assembly and demonstrates remarkable cytotoxicity, *MedChemComm*, 3 (2012) 720-724.
- [24] Z. Chen, A. Maderna, S.C. Sukuru, M. Wagenaar, C.J. O'Donnell, M.H. Lam, S. Musto, F. Loganzo, New cytotoxic benzosuberene analogs. Synthesis, molecular modeling and biological evaluation, *Bioorg. Med. Chem. Lett.* 23 (2013) 6688-6694.
- [25] Z. Chen, C.J. O'Donnell, A. Maderna, Synthesis of 3-methoxy-9-(3,4,5-trimethoxyphenyl)-6,7-dihydro-5H-benzo[7]annulen-4-ol, a potent antineoplastic benzosuberene derivative for anti-cancer chemotherapy, *Tetrahedron Lett.* 53 (2012) 64-66.
- [26] M.T. MacDonough, T.E. Strecker, E. Hamel, J.J. Hall, D.J. Chaplin, M.L.

Trawick, K.G. Pinney, Synthesis and biological evaluation of indole-based, anti-cancer agents inspired by the vascular disrupting agent 2-(3'-hydroxy-4'-methoxyphenyl)-3-(3',4',5'-trimethoxybenzoyl)-6-methoxyindole (OXi8006), *Bioorg. Med. Chem.* 21 (2013) 6831-6843.

[27] H. Zhou, R.R. Hallac, R. Lopez, R. Denney, M.T. MacDonough, L. Li, L. Liu, E.E. Graves, M.L. Trawick, K.G. Pinney, R.P. Mason, Evaluation of tumor ischemia in response to an indole-based vascular disrupting agent using BLI and (19)F MRI, *Am. J. Nucl. Med. and Mol. Imaging* 5 (2015) 143-153.

[28] D. Sunil, P.R. Kamath, Indole based tubulin polymerization inhibitors: an update on recent developments, *Mini Rev. Med. Chem.* (2016) Epub ahead of print.

[29] R. Patil, S.A. Patil, K.D. Beaman, S.A. Patil, Indole molecules as inhibitors of tubulin polymerization: potential new anticancer agents, an update (2013–2015), *Future Med. Chem.* 8 (2016) 1291-1316.

[30] K.R. Hadimani MB, Kautz JA, Ghatak A, Shirali AR, O'Dell H, Garner CM, Pinney KG., 2-(3-tert-Butyldimethylsiloxy-4-methoxyphenyl)-6-methoxy-3-(3,4,5-trimethoxybenzoyl)indole, *Acta Crystallogr C.* 58(2002) 330-332.

[31] T.E. Strecker, S.O. Odutola, R. Lopez, M.S. Cooper, J.K. Tidmore, A.K. Charlton-Sevcik, L. Li, M.T. MacDonough, M.B. Hadimani, A. Ghatak, L. Liu, D.J. Chaplin, R.P. Mason, K.G. Pinney, M.L. Trawick, The vascular disrupting activity of OXi8006 in endothelial cells and its phosphate prodrug OXi8007 in breast tumor xenografts, *Cancer Lett.* 369 (2015) 229-241.

[32] J. Yan, Y. Pang, J. Sheng, Y. Wang, J. Chen, J. Hu, L. Huang, X. Li, A novel synthetic compound exerts effective anti-tumour activity in vivo via the inhibition of tubulin polymerisation in A549 cells, *Biochem. Pharmacol.* 97 (2015) 51-61.

[33] J. Chen, J. Yan, J. Hu, Y. Pang, L. Huang, X. Li, Synthesis, biological evaluation and mechanism study of chalcone analogues as novel anti-cancer agents, *RSC Adv.* 5 (2015) 68128-68135.

[34] J. Yan, J. Chen, S. Zhang, J. Hu, L. Huang, X. Li, Synthesis, evaluation, and mechanism study of novel indole-chalcone derivatives exerting effective antitumor

activity through microtubule destabilization in vitro and in vivo, *J. Med. Chem.* 59 (2016) 5264-5283.

[35] M.-J. Lai, H.-L. Huang, S.-L. Pan, Y.-M. Liu, C.-Y. Peng, H.-Y. Lee, T.-K. Yeh, P.-H. Huang, C.-M. Teng, C.-S. Chen, Synthesis and biological evaluation of 1-arylsulfonyl-5-(N-hydroxyacrylamide) indoles as potent histone deacetylase inhibitors with antitumor activity in vivo, *J. Med. Chem.* 55 (2012) 3777-3791.

[36] C.K. Tan, L. Zhou, Y.-Y. Yeung, Aminothiobarbamide-catalyzed asymmetric bromolactonization of 1, 2-disubstituted olefinic acids, *Org. Lett.* 13 (2011) 2738-2741.

[37] J.F. Diaz, J.M. Andreu, Assembly of purified GDP-tubulin into microtubules induced by taxol and taxotere: reversibility, ligand stoichiometry, and competition, *Biochemistry*, 32 (1993) 2747-2755.

[38] D. Hanahan, R.A. Weinberg, The hallmarks of cancer, *Cell*, 100 (2000) 57-70.

[39] S.C. Ems-McClung, C.E. Walczak, Kinesin-13s in mitosis: Key players in the spatial and temporal organization of spindle microtubules, *Semin. Cell Dev. Biol.* 21 (2010) 276-282.

[40] C. Dominguez-Brauer, Kelsie L. Thu, Jacqueline M. Mason, H. Blaser, Mark R. Bray, Tak W. Mak, Targeting mitosis in cancer: emerging strategies, *Mol. Cell*, 60 (2015) 524-536.

[41] P.E. Eaton, G.R. Carlson, J.T. Lee, Phosphorus pentoxide-methanesulfonic acid. Convenient alternative to polyphosphoric acid, *J. Org. Chem.* 38 (1973) 4071-4073.

[42] M.S.C. Pedras, D.P.O. Okinyo, Syntheses of perdeuterated indoles and derivatives as probes for the biosyntheses of crucifer phytoalexins, *J. Labelled. Compd. Rad.* 49 (2006) 33-45.

[43] L.N. Ferguson, The synthesis of aromatic aldehydes, *Chem. Rev.* 38 (1946) 227-254.

[44] C. Lu, Y. Guo, J. Yan, Z. Luo, H.B. Luo, M. Yan, L. Huang, X. Li, Design, synthesis, and evaluation of multitarget-directed resveratrol derivatives for the treatment of Alzheimer's disease, *J. Med. Chem.* 56 (2013) 5843-5859.

[45] M.S.C. Pedras, E.E. Yaya, Dissecting metabolic puzzles through isotope feeding:

a novel amino acid in the biosynthetic pathway of the cruciferous phytoalexins rapalexin A and isocyaalexin A, *Org. Biomol. Chem.* 11 (2013) 1149-1166.

[46] R. Álvarez, P. Puebla, J.F. Díaz, A.C. Bento, R. García-Navas, J. de la Iglesia-Vicente, F. Mollinedo, J.M. Andreu, M. Medarde, R. Peláez, Endowing indole-based tubulin inhibitors with an anchor for derivatization: highly potent 3-substituted indolephenstatins and indoleisocombretastatins, *J. Med. Chem.* 56 (2013) 2813-2827.

[47] J.R. Peterson, M.E. Russell, I.B. Surjasasmita, Synthesis and experimental ionization energies of certain (E)-3-arylpropenoic acids and their methyl esters, *J. Chem. Eng. Data*, 33 (1988) 534-537.

Figure captions

Figure 1. Structures of the representative tubulin polymerization inhibitors and vascular disrupting agents (VDAs).

Figure 2. Disruption effect of compound **20** on the cellular microtubule network (A) and cell mitosis (B) visualized by immunofluorescence. A549 cells were plated in confocal dishes and exposed to **20** at the indicated concentrations for 24 h. Then, the cells were fixed and processed to study the immunofluorescence of microtubules (stained with primary β -tubulin mouse antibody and Alexa Fluor 488 goat anti-mouse IgG antibody, green) and nuclei (stained with Hoechst 33342, blue) using an LSM 570 laser confocal microscope (Carl Zeiss, Germany) as described in the Experimental Section. Magnification: $\times 64$ (A), $\times 100$ (B). The experiments were performed three times, and the results of representative experiments are shown.

Figure 3. Compound **20** arrested cell cycle progression at the G₂/M phase in a dose- and time-dependent manner. The A549 cells were treated with compound **20** at 10, 20, or 50 nM for 24 h (A) or 48 h (B). Quantitative analysis of the percentage of cells in each cell cycle phase were analysed by EXPO32 ADC analysis software. The experiments were performed three times, and the results of representative experiments are shown.

Figure 4. Compound **20** induced A549 cell apoptosis in a dose- and time-dependent manner. The A549 cells were treated with compound **20** at 10, 20, or 50 nM for 24 h (A) or 48 h (B). The percentages of cells in each stage of cell apoptosis were quantified by flow cytometry: (upper left quadrant) necrosis cells; (upper right quadrant) late-apoptotic cells; (bottom left quadrant) live cells; and (bottom right quadrant) early apoptotic cells. The experiments were performed three times, and the

results of representative experiments are shown.

Table captions

Table 1. Antiproliferative activity of compounds against seven human cancer cell lines^a

Table 2. Effects of the selected compounds on tubulin polymerization inhibition

Table 3. The selectivity ratio of compound **20** toward human normal cells and cancer cells.

Scheme captions

Scheme 1. Reagents and conditions: (a) benzenesulfonyl chloride, KOH, TBAHS, CH₂Cl₂, room temperature; (b) (i) (3-carboxypropyl)triphenylphosphonium bromide, NaHMDS, THF, -20 °C; (ii) aldehyde, **6**, -78 °C, 18 h; (c) Pd/C, H₂, MeOH; (d) Eaton's Reagent: 7.7% (w/w) P₂O₅ in methanesulfonic acid, room temperature; (e) (i) 5-bromo-1,2,3-trimethoxybenzene, n-BuLi, THF; (ii) ketone, **9**, -78 °C, 12 h; (f) p-toluenesulfonic acid, CHCl₃; (g) 1 M KOH, MeOH; (h) CH₃I / C₂H₅Br / C₃H₇Br, NaH, THF; (i) NaBH₃CN, CH₃COOH; (j) Hexamethylenetetramine, CH₃COOH, N₂.

Scheme 2. Reagents and conditions: (a) Hexamethylenetetramine, CH₃COOH, N₂; (b) (i) oxalyl chloride, Et₂O; (ii) CH₃OH, Et₃N; (c) H₂, Pd/C, CH₃OH; (d) NaBH₄, CH₃OH.

Scheme 3. Reagents and conditions: (a) malonic acid, piperidine, pyridine; (b) Pd/C, H₂, MeOH; (c) methanesulfonic acid, P₂O₅, room temperature; (d) 1 M KOH, MeOH; (e) CH₃I, NaH, THF; (f) (i) 5-bromo-1,2,3-trimethoxybenzene, n-BuLi, THF; (ii) ketone, **25**, -78 °C, 12 h.

Highlights:

1. A new series of cyclic-indole analogues as anti-tumour agents were synthesized.
2. Most compounds showed potent cytotoxicity and tubulin polymerization inhibition.
3. Compound **20** arrested cell cycle and induced apoptosis in A549 cells.